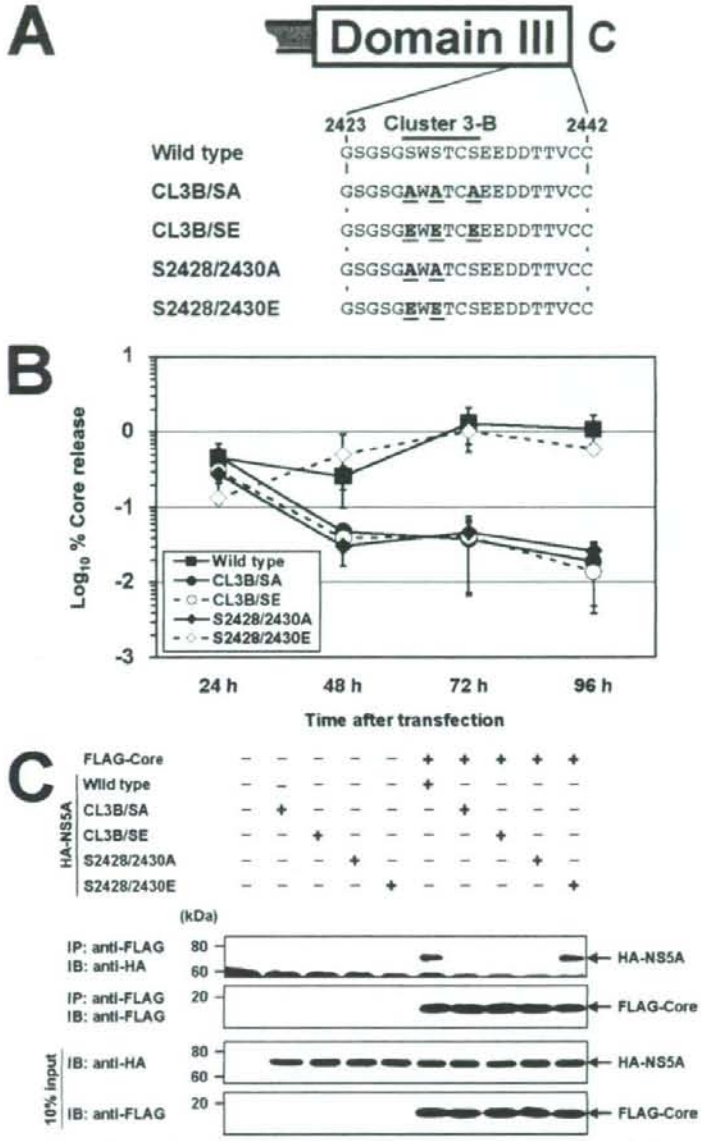

FIG. 6. Effect of glutamic acid substitutions for phosphoserines at aa 2428, 2430, and 2433 on virus production and the interaction of NS5A with the core protein. (A) Alanine or glutamic acid substitutions for serine residues at aa 2428, 2430, and 2433. The numbers indicate amino acid positions within the polyprotein of the JFH-1 isolate. The names shown on the left represent full-length HCV or N-terminally HA-tagged NS5A constructs used in this experiment. Amino acid substitutions are marked in bold and underlined. C represents the C terminus. (B) Effect of alanine or glutamic acid substitutions on virus production. After transfection of in vitro transcripts of the HCV genomes specified in the inset into Huh-7 cells, the cells and the culture supernatants were harvested at the time points given, and the amounts of core protein were determined by core protein-specific ELISA. Percent core protein release (vertical axis) indicates the percentage of released core protein in relation to total core protein (the sum of intra- and extracellular core protein) calculated for each time point. Mean values and standard deviations for at least triplicate experiments are shown. (C) Effect of alanine or glutamic acid substitutions on the interaction between NS5A and the core protein. N-terminally FLAG-tagged core protein and N-terminally HA-tagged NS5A carrying defined mutations were coexpressed in Huh-7 cells and immunoprecipitated with anti-FLAG antibody. The resulting precipitates were examined by immunoblotting (IB) using anti-HA or FLAG antibody. One-tenth of the cell lysates used in IP is as shown as the 10% input.

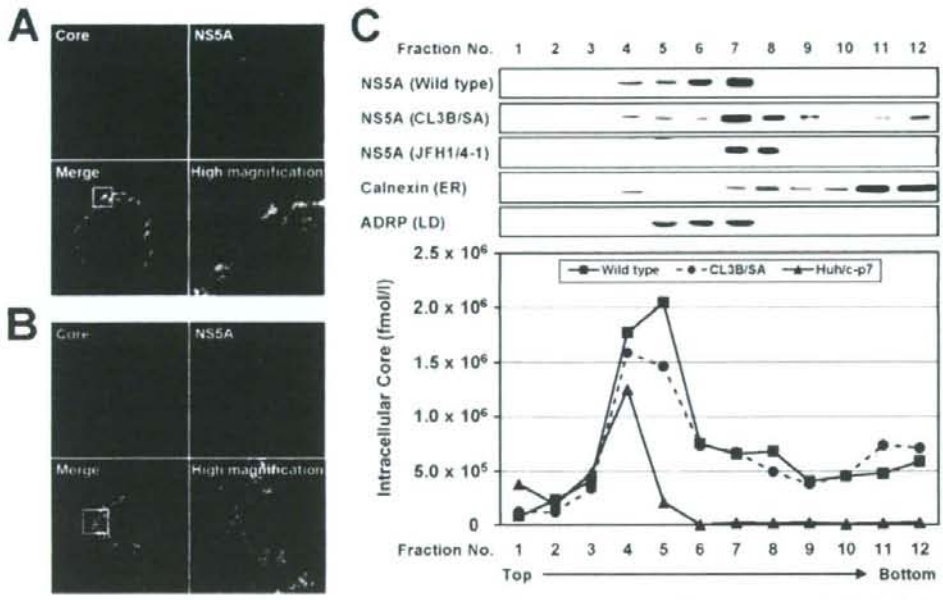

FIG. 7. Subcellular localization of NS5A and the core protein in HCV-replicating cells. Huh-7 cells were transfected with the in vitro transcript of the HCV genome, wild type (A) or CL3B/SA (B). Seventy-two hours after transfection, the cells were fixed with 4% paraformaldehyde, permeabilized with 0.3% Triton X-100, and double stained with antibodies against the core protein (green) and NS5A (red), followed by staining with an Alexa Fluor 488- or Alexa Fluor 555-conjugated antibody. High-magnification panels are enlarged images of white squares in the merge panels. (C) HCV (wild type or CL3B/SA)-replicating cells, JFH1/4-1 cells harboring a subgenomic replicon of JFH-1, or Huh/c-p7 cells stably expressing JFH-1 structural proteins were lysed by freeze-thawing, and the cell lysates were fractionated on 5 to 25% iodixanol gradients. The distributions of NS5A, calnexin (ER marker), and ADRP (LD marker) were determined by immunoblotting, and those of the core protein were examined by core protein-specific ELISA.

(50). However, the mechanism by which NS proteins participate in virus assembly or the role of the interaction between structural and NS proteins in virus life cycles has not been fully elucidated. Here, we have clearly demonstrated that HCV NS5A interacts with the core protein in coimmunoprecipitation experiments not only with coexpression of each epitope-tagged protein but also with cells expressing the viral genome; and by using immunofluorescence and subcellular fractionation analysis, we have confirmed that mutations in CL3B abolish colocalization of NS5A and the core protein, presumably around LDs. In addition, the intracellular infectivity assay and IP-RT-PCR strongly suggest that impairment of the NS5A-core protein interaction results in disruption of virus production at an early stage of virion assembly. On the basis of the present results and findings in accompanying articles, one may infer the following events: newly synthesized HCV RNAs bound to NS5A are released from the replication complex-containing membrane compartment and can be captured by the core protein via interaction with domain III of NS5A at the surface of LDs or LD-associated membranes. Consequently, the viral RNAs are encapsidated, and virion assembly proceeds in the local environment. Recruitment of newly synthesized viral RNAs to the core protein could be important for efficient nucleocapsid formation in cells, where concentrations of the viral genome and the structural proteins are typically low, and may contribute to the selection of the viral genome to be packaged. Interaction between NS5A and the core protein has been previously reported, and the NS5A region containing an interferon sensitivity determining region and the PKR-binding sequence (aa 2212 to 2330) has been mapped to that required for binding with core protein by yeast two-hybrid and in vitro pull-down assays (13). However, involvement of domain III in the NS5A-core protein interaction was not analyzed in detail, and a role for the NS5A-core protein interaction in the HCV life cycle was not examined in that study.

A growing body of evidence points to phosphorylation of NS5A as being important in controlling HCV RNA replication. Although the degree and the requirement for its hyperphosphorylation diverge between different HCV isolates, mutations that are associated with increased replicative fitness of HCV replicons frequently lead to a reduced level of NS5A hyperphosphorylation (1, 5, 36). Inhibitors of serine/threonine protein kinases that block NS5A hyperphosphorylation facilitate replication of a non-culture-adapted replicon (3, 36). One model that has been proposed suggests that NS5A hyperphosphorylation negatively regulates HCV RNA replication by disrupting the interaction between NS5A and the vesicle-associated membrane protein-associated protein subtype A, a cellular factor considered necessary for efficient RNA replication (5). However, the regulatory role of the basal phosphorylation of NS5A in the viral life cycle is poorly understood. It has been reported that the C-terminal region of NS5A (aa 2350 to 2419)

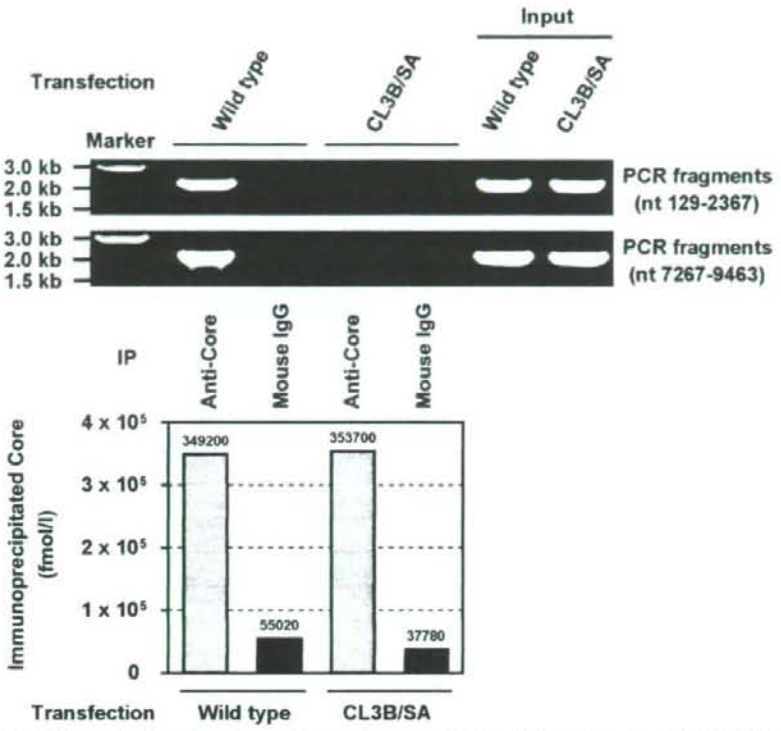

FIG. 8. IP-RT-PCR of HCV-replicating cells performed to examine the association between the core protein and the HCV genome RNA. Huh-7 cells were transfected with the in vitro transcript of the HCV genome (wild type or CL3B/SA) and lysed in 500 μl of hypotonic buffer at 72 h posttransfection. After IP with an anti-core protein antibody or mouse IgG, immunoprecipitates were eluted in 100 μl of elution buffer. RNAs in immunocomplexes were isolated by acid guanidinium thiocyanate-phenol-chloroform extraction. PCR was carried out as described in Materials and Methods with primer sets amplifying the fragments of nt 129 to 2367 and nt 7267 to 9463 of the JFH-1 genome. One-tenth (10 μl) of each eluted immunoprecipitate was used for assays of the core protein amounts to ensure IP efficiency (lower panel). RNA extracted from a small aliquot of each cell lysate used in IP-RT-PCR is shown as the input.

is involved in basal phosphorylation (23). There are highly conserved serine residues in this region, and alanine substitutions or in-frame deletion of the serine residues has been shown to impair basal phosphorylation but not to affect RNA replication in the genotype 1b isolate (1). Consistently, a metabolic ^{32}P labeling experiment in the present study demonstrated that NS5A mutants of the JFH-1 isolate in the region impair the basal phosphorylation. Nevertheless, Tellinghuisen et al. noted that the serine at aa 2433 of JFH-1 is involved in generating hyperphosphorylated NS5A, as shown by Western blotting (50). The basis for this difference is uncertain. To date, there is no clear evidence to determine which serine residues located in domain III are phosphoacceptor sites or whether these residues influence NS5A phosphorylation in an indirect fashion. Future study to map phosphoacceptor sites in the NS5A domain III by biochemical approaches is needed.

We found that two of the three serine residues at CL3B are responsible for regulating the interaction of NS5A with the core protein as well as for infectious virus production. To further evaluate the effect of constitutive serine phosphorylation at the cluster, we replaced the serine residues with glutamic acid, which mimics the presence of phosphoserines. The S2428/2430E mutant led to restoration of the interaction of NS5A with the core protein and virus production up to levels similar to the wild type. Somewhat unexpectedly, the triple glutamic acid substitution (CL3B/SE) exhibited only a slight restoration effect or none at all. It is considered that the degree of negative charge on the glutamic acid residue is not completely equivalent to that of phosphoserine. It is likely that the range of acidity at the local environment of the NS5A domain III that will allow interaction with the core protein is rather narrow. Induction of a conformational change in NS5A by the incorporation of phosphate may also be important for its interaction with the core protein. Tellinghuisen et al. reported that a single serine-to-alanine substitution at aa 2433 blocks the production of infectious virus and that casein kinase II likely phosphorylates the residue (50). Although this seems inconsistent with our results, these investigators also showed that deletions producing a lack of all three serine residues in the cluster inhibited virus production more severely than a single mutation. We observed that a single substitution of S2428A, S2430A, or S2433A resulted in a moderate decrease

in the virus released from the transfected cells; however, more evident perturbation was obtained from double or triple substitutions (Fig. 5A and B). Tellinghuisen et al. determined the HCV production at 48 h after RNA transfection and found a marked inhibition by the single substitution S2433A. In our study, as indicated in Fig. 5A, the reduction caused by the S2433A mutant was approximately 90% at 48 h after transfection; however, the virus production from the mutant reached a similar level to that of the wild type at 96 h posttransfection.

Several previous studies have found that apolipoproteins B (apoB) and E (apoE), microsomal triglyceride transfer protein, and HCV p7 protein are key factors for production of the infectious HCV particles (4, 11, 16, 22, 47). Assembly and maturation of the viral particles appear to depend on the formation of very-low-density lipoprotein, a large particle containing apoB, apoE, and large amounts of neutral lipids in hepatic cells. p7 protein is primarily involved in a late step of virus particle production, and the findings support the idea that p7 acts as viroporin, which has the capacity to compromise cell membrane integrity and thus favors the release of viral progeny. How the early step in virion production regulated by the NS5A-core protein interaction links with the later step(s) involved in the very-low-density lipoprotein assembly or p7 function remains an interesting question to be addressed.

In summary, we demonstrated that the C-terminal serine cluster of NS5A (aa 2428, 2430, and 2433), which is involved in generating the basal phosphorylated form, is a determinant of NS5A interaction with the core protein and the subcellular localization of NS5A. Mutation of this cluster blocks the NS5A-core protein interaction, resulting in perturbation of association between the core protein and HCV RNA. It is thus tempting to consider that NS5A plays a key role in transporting the viral genome RNA synthesized by the replication complex to the surface of LDs or LD-associated membranes, where the core protein localizes, leading to facilitation of nucleocapsid formation. Structural analysis of the NS5A domain III-core protein complex should provide greater insight into the mode of interaction between these viral proteins. Identification of residues at the interface that are involved in important interactions will be of significant value in designing novel structure-based inhibitors to block the early step of HCV particle formation.

ACKNOWLEDGMENTS

We are grateful to Francis V. Chisari (The Scripps Research Institute) for providing Huh-7 cells. We thank M. Matsuda, S. Yoshizaki, T. Shimoji, M. Kaga, and M. Sasaki for technical assistance and T. Mizoguchi for secretarial work.

This work was supported by Grants-in-Aid from the Ministry of Health, Labor and Welfare; by the Program for Promotion of Fundamental Studies in Health Sciences of the Organization for Drug ADR Relief, R&D Promotion and Product Review of Japan (grant ID:01-3); by the Japan Society for the Promotion of Science; and by Research on Health Sciences focusing on Drug Innovation from the Japan Health Sciences Foundation, Japan. T.M. is the recipient of a Research Resident Fellowship from the Foundation for Promotion of Cancer Research in Japan.

REFERENCES

1. **Appel, N., T. Pietschmann, and R. Bartenschlager.** 2005. Mutational analysis of hepatitis C virus nonstructural protein 5A: potential role of differential phosphorylation in RNA replication and identification of a genetically flexible domain. J. Virol. **79:**3187–3194.
2. **Appel, N., M. Zayas, S. Miller, J. Krijnse-Locker, T. Schaller, P. Friebe, S. Kallis, U. Engel, and R. Bartenschlager.** 2008. Essential role of domain III of nonstructural protein 5A for hepatitis C virus infectious particle assembly. PLoS Pathog. **4:**e1000035.
3. **Bürckstümmer, T., M. Kriegs, J. Lupberger, E. K. Pauli, S. Schmittel, and E. Hildt.** 2006. Raf-1 kinase associates with hepatitis C virus NS5A and regulates viral replication. FEBS Lett. **580:**575–580.
4. **Chang, K. S., J. Jiang, Z. Cai, and G. Luo.** 2007. Human apolipoprotein E is required for infectivity and production of hepatitis C virus in cell culture. J. Virol. **81:**13783–13793.
5. **Evans, M. J., C. M. Rice, and S. P. Goff.** 2004. Phosphorylation of hepatitis C virus nonstructural protein 5A modulates its protein interactions and viral RNA replication. Proc. Natl. Acad. Sci. USA **101:**13038–13043.
6. **Gale, M., Jr., C. M. Blakely, B. Kwieciszewski, S. L. Tan, M. Dossett, N. M. Tang, M. J. Korth, S. J. Polyak, D. R. Gretch, and M. G. Katze.** 1998. Control of PKR protein kinase by hepatitis C virus nonstructural 5A protein: molecular mechanisms of kinase regulation. Mol. Cell. Biol. **18:**5208–5218.
7. **Gale, M., Jr., and M. G. Katze.** 1998. Molecular mechanisms of interferon resistance mediated by viral-directed inhibition of PKR, the interferon-induced protein kinase. Pharmacol. Ther. **78:**29–46.
8. **Gale, M., Jr., B. Kwieciszewski, M. Dossett, H. Nakao, and M. G. Katze.** 1999. Antiapoptotic and oncogenic potentials of hepatitis C virus are linked to interferon resistance by viral repression of the PKR protein kinase. J. Virol. **73:**6506–6516.
9. **Gale, M. J., Jr., M. J. Korth, and M. G. Katze.** 1998. Repression of the PKR protein kinase by the hepatitis C virus NS5A protein: a potential mechanism of interferon resistance. Clin. Diagn. Virol. **10:**157–162.
10. **Gale, M. J., Jr., M. J. Korth, N. M. Tang, S. L. Tan, D. A. Hopkins, T. E. Dever, S. J. Polyak, D. R. Gretch, and M. G. Katze.** 1997. Evidence that hepatitis C virus resistance to interferon is mediated through repression of the PKR protein kinase by the nonstructural 5A protein. Virology **230:**217–227.
11. **Gastaminza, P., G. Cheng, S. Wieland, J. Zhong, W. Liao, and F. V. Chisari.** 2008. Cellular determinants of hepatitis C virus assembly, maturation, degradation, and secretion. J. Virol. **82:**2120–2129.
12. **Gastaminza, P., S. B. Kapadia, and F. V. Chisari.** 2006. Differential biophysical properties of infectious intracellular and secreted hepatitis C virus particles. J. Virol. **80:**11074–11081.
13. **Goh, P. Y., Y. J. Tan, S. P. Lim, S. G. Lim, Y. H. Tan, and W. J. Hong.** 2001. The hepatitis C virus core protein interacts with NS5A and activates its caspase-mediated proteolytic cleavage. Virology **290:**224–236.
14. **Hicke, L., B. Zanolari, and H. Riezman.** 1998. Cytoplasmic tail phosphorylation of the alpha-factor receptor is required for its ubiquitination and internalization. J. Cell Biol. **141:**349–358.
15. **Hoofnagle, J. H.** 2002. Course and outcome of hepatitis C. Hepatology **36:**S21–S29.
16. **Huang, H., F. Sun, D. M. Owen, W. Li, Y. Chen, M. Gale, Jr., and J. Ye.** 2007. Hepatitis C virus production by human hepatocytes dependent on assembly and secretion of very low-density lipoproteins. Proc. Natl. Acad. Sci. USA **104:**5848–5853.
17. **Huang, L., J. Hwang, S. D. Sharma, M. R. Hargittai, Y. Chen, J. J. Arnold, K. D. Raney, and C. E. Cameron.** 2005. Hepatitis C virus nonstructural protein 5A (NS5A) is an RNA-binding protein. J. Biol. Chem. **280:**36417–36428.
18. **Ishii, K., K. Murakami, S. S. Hmwe, B. Zhang, J. Li, M. Shirakura, K. Morikawa, R. Suzuki, T. Miyamura, T. Wakita, and T. Suzuki.** 2008. Trans-encapsidation of hepatitis C virus subgenomic replicon RNA with viral structure proteins. Biochem. Biophys. Res. Commun. **371:**446–450.
19. **Ishii, K., Y. Ueda, K. Matsuo, Y. Matsuura, T. Kitamura, K. Kato, Y. Izumi, K. Someya, T. Ohsu, M. Honda, and T. Miyamura.** 2002. Structural analysis of vaccinia virus DIs strain: application as a new replication-deficient viral vector. Virology **302:**433–444.
20. **Jesch, S. A., A. J. Mehta, M. Velliste, R. F. Murphy, and A. D. Linstedt.** 2001. Mitotic Golgi is in a dynamic equilibrium between clustered and free vesicles independent of the ER. Traffic **2:**873–884.
21. **Johnson, R. F., S. E. McCarthy, P. J. Godlewski, and R. N. Harty.** 2006. Ebola virus VP35-VP40 interaction is sufficient for packaging 3E–5E minigenome RNA into virus-like particles. J. Virol. **80:**5135–5144.
22. **Jones, C. T., C. L. Murray, D. K. Eastman, J. Tassello, and C. M. Rice.** 2007. Hepatitis C virus p7 and NS2 proteins are essential for production of infectious virus. J. Virol. **81:**8374–8383.
23. **Kaneko, T., Y. Tanji, S. Satoh, M. Hijikata, S. Asabe, K. Kimura, and K. Shimotohno.** 1994. Production of two phosphoproteins from the NS5A region of the hepatitis C viral genome. Biochem. Biophys. Res. Commun. **205:**320–326.
24. **Kato, T., T. Date, M. Miyamoto, M. Sugiyama, Y. Tanaka, E. Orito, T. Ohno, K. Sugihara, I. Hasegawa, K. Fujiwara, K. Ito, A. Ozasa, M. Mizokami, and T. Wakita.** 2005. Detection of anti-hepatitis C virus effects of interferon and ribavirin by a sensitive replicon system. J. Clin. Microbiol. **43:**5679–5684.
25. **Kümmerer, B. M., and C. M. Rice.** 2002. Mutations in the yellow fever virus nonstructural protein NS2A selectively block production of infectious particles. J. Virol. **76:**4773–4784.

26. **Leung, J. Y., G. P. Pijlman, N. Kondratieva, J. Hyde, J. M. Mackenzie, and A. A. Khromykh.** 2008. Role of nonstructural protein NS2A in flavivirus assembly. J. Virol. **82:**4731–4741.
27. **Liang, T. J., B. Rehermann, L. B. Seeff, and J. H. Hoofnagle.** 2000. Pathogenesis, natural history, treatment, and prevention of hepatitis C. Ann. Intern. Med. **132:**296–305.
28. **Lindenbach, B. D., M. J. Evans, A. J. Syder, B. Wolk, T. L. Tellinghuisen, C. C. Liu, T. Maruyama, R. O. Hynes, D. R. Burton, J. A. McKeating, and C. M. Rice.** 2005. Complete replication of hepatitis C virus in cell culture. Science **309:**623–626.
29. **Liu, W. J., H. B. Chen, and A. A. Khromykh.** 2003. Molecular and functional analyses of Kunjin virus infectious cDNA clones demonstrate the essential roles for NS2A in virus assembly and for a nonconservative residue in NS3 in RNA replication. J. Virol. **77:**7804–7813.
30. **Liu, W. J., P. L. Sedlak, N. Kondratieva, and A. A. Khromykh.** 2002. Complementation analysis of the flavivirus Kunjin NS3 and NS5 proteins defines the minimal regions essential for formation of a replication complex and shows a requirement of NS3 in *cis* for virus assembly. J. Virol. **76:**10766–10775.
31. **Manns, M. P., H. Wedemeyer, and M. Cornberg.** 2006. Treating viral hepatitis C: efficacy, side effects, and complications. Gut **55:**1350–1359.
32. **Miyamoto, M., T. Kato, T. Date, M. Mizokami, and T. Wakita.** 2006. Comparison between subgenomic replicons of hepatitis C virus genotypes 2a (JFH-1) and 1b (Con1 NK5.1). Intervirology **49:**37–43.
33. **Miyanari, Y., K. Atsuzawa, N. Usuda, K. Watashi, T. Hishiki, M. Zayas, R. Bartenschlager, T. Wakita, M. Hijikata, and K. Shimotohno.** 2007. The lipid droplet is an important organelle for hepatitis C virus production. Nat. Cell Biol. **9:**1089–1097.
34. **Moradpour, D., M. J. Evans, R. Gosert, Z. Yuan, H. E. Blum, S. P. Goff, B. D. Lindenbach, and C. M. Rice.** 2004. Insertion of green fluorescent protein into nonstructural protein 5A allows direct visualization of functional hepatitis C virus replication complexes. J. Virol. **78:**7400–7409.

34a. **Murakami, K., T. Kimura, M. Osaki, K. Ishii, T. Miyamura, T. Suzuki, T. Wakita, and I. Shoji.** 2008. Virological characterization of the hepatitis C virus JFH-1 strain in lymphocytic cell lines. J. Gen. Virol. **89:**1587–1592.

35. **National Institutes of Health.** 2002. NIH consensus statement on management of hepatitis C. NIH Consens. State. Sci. Statements **19:**1–46.
36. **Neddermann, P., M. Quintavalle, C. Di Pietro, A. Clementi, M. Cerretani, S. Altamura, L. Bartholomew, and R. De Francesco.** 2004. Reduction of hepatitis C virus NS5A hyperphosphorylation by selective inhibition of cellular kinases activates viral RNA replication in cell culture. J. Virol. **78:**13306–13314.
37. **Niwa, H., K. Yamamura, and J. Miyazaki.** 1991. Efficient selection for high-expression transfectants with a novel eukaryotic vector. Gene **108:**193–199.
38. **Pawlotsky, J. M.** 1999. Hepatitis C virus (HCV) NS5A protein: role in HCV replication and resistance to interferon-alpha. J. Viral Hepat. **6**(Suppl. 1)**:** 47–48.
39. **Pawlotsky, J. M., G. Germanidis, A. U. Neumann, M. Pellerin, P. O. Frainais, and D. Dhumeaux.** 1998. Interferon resistance of hepatitis C virus genotype 1b: relationship to nonstructural 5A gene quasispecies mutations. J. Virol. **72:**2795–2805.
40. **Poynard, T., M. F. Yuen, V. Ratziu, and C. L. Lai.** 2003. Viral hepatitis C. Lancet **362:**2095–2100.
41. **Schaller, T., N. Appel, G. Koutsoudakis, S. Kallis, V. Lohmann, T. Pietschmann, and R. Bartenschlager.** 2007. Analysis of hepatitis C virus superinfection exclusion by using novel fluorochrome gene-tagged viral genomes. J. Virol. **81:**4591–4603.
42. **Seeff, L. B., and J. H. Hoofnagle.** 2003. Appendix: The National Institutes of Health Consensus Development Conference: management of hepatitis C 2002. Clin. Liver Dis. **7:**261–287.
43. **Seeff, L. B., and J. H. Hoofnagle.** 2002. National Institutes of Health Consensus Development Conference: management of hepatitis C: 2002. Hepatology **36:**S1–S2.
44. **Shavinskaya, A., S. Boulant, F. Penin, J. McLauchlan, and R. Bartenschlager.** 2007. The lipid droplet binding domain of hepatitis C virus core protein is a major determinant for efficient virus assembly. J. Biol. Chem. **282:**37158–37169.
45. **Shi, S. T., S. J. Polyak, H. Tu, D. R. Taylor, D. R. Gretch, and M. M. Lai.** 2002. Hepatitis C virus NS5A colocalizes with the core protein on lipid droplets and interacts with apolipoproteins. Virology **292:**198–210.
46. **Shirakura, M., K. Murakami, T. Ichimura, R. Suzuki, T. Shimoji, K. Fukuda, K. Abe, S. Sato, M. Fukasawa, Y. Yamakawa, M. Nishijima, K. Moriishi, Y. Matsuura, T. Wakita, T. Suzuki, P. M. Howley, T. Miyamura, and I. Shoji.** 2007. E6AP ubiquitin ligase mediates ubiquitylation and degradation of hepatitis C virus core protein. J. Virol. **81:**1174–1185.
47. **Steinmann, E., F. Penin, S. Kallis, A. H. Patel, R. Bartenschlager, and T. Pietschmann.** 2007. Hepatitis C virus p7 protein is crucial for assembly and release of infectious virions. PLoS Pathog. **3:**e103.
48. **Tan, S. L., and M. G. Katze.** 2001. How hepatitis C virus counteracts the interferon response: the jury is still out on NS5A. Virology **284:**1–12.
49. **Tanji, Y., T. Kaneko, S. Satoh, and K. Shimotohno.** 1995. Phosphorylation of hepatitis C virus-encoded nonstructural protein NS5A. J. Virol. **69:**3980–3986.
50. **Tellinghuisen, T. L., K. L. Foss, and J. Treadaway.** 2008. Regulation of hepatitis C virion production via phosphorylation of the NS5A protein. PLoS Pathog. **4:**e1000032.
51. **Tellinghuisen, T. L., K. L. Foss, J. C. Treadaway, and C. M. Rice.** 2008. Identification of residues required for RNA replication in domains II and III of the hepatitis C virus NS5A protein. J. Virol. **82:**1073–1083.
52. **Tellinghuisen, T. L., J. Marcotrigiano, A. E. Gorbalenya, and C. M. Rice.** 2004. The NS5A protein of hepatitis C virus is a zinc metalloprotein. J. Biol. Chem. **279:**48576–48587.
53. **Tellinghuisen, T. L., J. Marcotrigiano, and C. M. Rice.** 2005. Structure of the zinc-binding domain of an essential component of the hepatitis C virus replicase. Nature **435:**374–379.
54. **van den Hoff, M. J., A. F. Moorman, and W. H. Lamers.** 1992. Electroporation in "intracellular" buffer increases cell survival. Nucleic Acids Res. **20:**2902.
55. **van Regenmortel, M. H. V., C. M. Fauquet, D. H. L. Bishop, E. B. Carstens, M. K. Estes, S. M. Lemon, J. Maniloff, M. A. Mayo, D. J. McGeoch, C. R. Pringle, and R. B. Wickner (ed.).** 2000. Virus taxonomy: classification and nomenclature of viruses. Seventh report of the International Committee on Taxonomy of Viruses. Academic Press, San Diego, CA.
56. **Wakita, T., T. Pietschmann, T. Kato, T. Date, M. Miyamoto, Z. Zhao, K. Murthy, A. Habermann, H. G. Krausslich, M. Mizokami, R. Bartenschlager, and T. J. Liang.** 2005. Production of infectious hepatitis C virus in tissue culture from a cloned viral genome. Nat. Med. **11:**791–796.
57. **Watashi, K., M. Hijikata, A. Tagawa, T. Doi, H. Marusawa, and K. Shimotohno.** 2003. Modulation of retinoid signaling by a cytoplasmic viral protein via sequestration of Sp110b, a potent transcriptional corepressor of retinoic acid receptor, from the nucleus. Mol. Cell. Biol. **23:**7498–7509.
58. **Zhong, J., P. Gastaminza, G. Cheng, S. Kapadia, T. Kato, D. R. Burton, S. F. Wieland, S. L. Uprichard, T. Wakita, and F. V. Chisari.** 2005. Robust hepatitis C virus infection in vitro. Proc. Natl. Acad. Sci. USA **102:**9294–9299.

Virology 376 (2008) 397–407

Contents lists available at ScienceDirect

Virology

journal homepage: www.elsevier.com/locate/yviro

Intragenotypic JFH1 based recombinant hepatitis C virus produces high levels of infectious particles but causes increased cell death

Guaniri Mateu [a], Ruben O. Donis [b], Takaji Wakita [c], Jens Bukh [d,e,f], Arash Grakoui [a,*]

[a] Department of Medicine, Division of Infectious Diseases, Emory University School of Medicine, Atlanta GA 30329, USA
[b] Molecular Virology and Vaccines Branch, Centers for Disease Control and Prevention Atlanta, GA 30333, USA
[c] Department of Virology II, National Institute of Infectious Diseases, Shinjuku, Tokyo, 162-8640 Japan
[d] Department of Infectious Diseases and Clinical Research Center, Copenhagen University Hospital, DK-2650 Hvidovre, Denmark
[e] Department of International Health, Immunology and Microbiology, Faculty of Health Sciences, University of Copenhagen, DK-2200 Copenhagen N, Denmark
[f] Hepatitis Viruses Section, Laboratory of Infectious Diseases, National Institute of Allergy and Infectious Diseases, National Institutes of Health, Bethesda, MD 20892, USA

ARTICLE INFO

Article history:
Received 6 February 2008
Returned to author for revision
29 February 2008
Accepted 24 March 2008
Available online 2 May 2008

Keywords:
Hepatitis C virus
Intragenotypic recombinant
JFH
Cell death

ABSTRACT

The full-length hepatitis C virus (HCV) JFH1 genome (genotype 2a) produces moderate titers of infectious particles in cell culture but the optimal determinants required for virion production are unclear. It has been shown that intragenotypic recombinants encoding core to NS2 from J6CF in the context of JFH1 are more robust in the release of viral particles. To understand the contributions of structural and nonstructural genes to HCV replication potential and infectivity, we have characterized intragenotypic recombinant genotype 2a viruses with different portions of the J6 isolate engineered into the JFH1 infectious clone. All genomes produced high levels of intracellular HCV RNA and NS3 protein in Huh-7.5 transfected cells. However, JFH1 genomes containing J6 sequences from C to E2 (CE2) or C to p7 (Cp7) secreted up to 100-fold more infectious HCV particles than the parental JFH1 clone. Subsequent infection of naive Huh-7.5 cells with each of the J6/JFH1 recombinants at a multiplicity of infection of 0.0003 resulted in high viral titers only for CE2 and Cp7 viruses. Comparison of virion production by the Cp7 J6/JFH1 recombinant to previously described J6/JFH1 recombinants showed flexibility of the chimeric junction. Moreover, NTRNS2 a chimeric virus equivalent to the previously reported FL-J6/JFH chimera, showed a 10-fold enhancement of virus titers compared to CNS2. NTRNS2 differs from CNS2 by three nucleotide differences residing in the 5′ NTR and core coding sequence and all three nucleotide changes were necessary for increased virion production. Importantly, cells producing Cp7 virus showed increased apoptosis compared with JFH1, an effect correlating with virion production. These studies begin to unravel requirements for robust virus replication and the relationship between increased virion production and host cell viability.

Introduction

Hepatitis C virus (HCV) infection currently affects approximately 170 million people worldwide and is resolved by only a minority of patients (1999; Wasley and Alter, 2000). The chronic viral infection frequently progresses to end-stage liver disease, cirrhosis and in some cases, to development of hepatocellular carcinoma (Alter et al., 1999; Alter et al., 1992). There is no therapeutic or prophylactic vaccine available for HCV and the only effective antiviral therapy, interferon and ribavirin, produces sustained viral clearance in less than 50% of treated patients (Reichard et al., 1997).

A noteworthy characteristic of the HCV genome, a plus-strand RNA of ~9.6 kb, is its genetic diversity (Lindenbach and Rice, 2005; Moradpour et al., 2007). HCV isolates have been classified into six major genotypes (from 1–6) and multiple subtypes (a,b,c, etc.). In infected individuals, HCV exists as quasispecies of closely related genomes (Bukh et al., 1995). A number of studies have suggested that the outcome of HCV infection as well as the response to interferon treatment depends on the genotype or quasispecies with which the patient is infected. However, it is not clear how subtle differences in the HCV genome affect viral replication, infectivity and host response (Sakai et al., 2007).

Until recently, the only available system to study the replication cycle of HCV was the subgenomic replicons that were adapted for efficient RNA replication in vitro (Blight et al., 2000; Lohmann et al., 1999). However, full-length genomes containing cell culture-adaptive mutations did not produce infectious virus particles in culture and were severely attenuated in vivo (Bukh et al., 2002). These observations led to the hypothesis that mutations that enhance RNA replication may have deleterious effects on virion production. In 2003, Kato et al. reported that a subgenomic replicon derived from JFH1 cDNA did not require adaptive mutations for efficient replication in cell culture (Kato et al., 2003a). JFH1 is an HCV isolate of genotype 2a (GT2a) obtained from a patient with fulminant hepatitis (Kato et al., 2001). For reasons that are still not

* Corresponding author. Emory University School of Medicine, 954 Gatewood Road, NE, Atlanta, GA 30329, USA. Fax: +1 404 727 7768.
E-mail address: arash.grakoui@emory.edu (A. Grakoui).

0042-6822/$ – see front matter © 2008 Elsevier Inc. All rights reserved.
doi:10.1016/j.virol.2008.03.027

understood, the full-length JFH1 genome has been shown to produce moderate titers of infectious particles in cell culture (Wakita et al., 2005).

We sought to exploit the use of synthetic chimeric viruses to map the functional regions of HCV using viruses with different phenotypes. The infectious clone pJ6CF encodes the consensus polyprotein of HCV strain HC-J6 (CH) that belongs to genotype 2a, as does JFH1, but J6 does not replicate in the hepatoma cell line Huh-7.5 (Yanagi et al., 1999). Chimeric clones have recently been reported in which the structural region, p7, and NS2 of the JFH1 genome has been replaced with the analogous region from clones with the same or different genotypes (Gottwein et al., 2007; Lindenbach et al., 2005; Pietschmann et al., 2006; Yi et al., 2007). Intragenotypic chimeric viruses in which the structural region, p7 and a portion of NS2 from HCV JFH1 was replaced with the corresponding region from the infectious clone pJ6CF derived from the HCV strain HC-J6(CH), exhibited enhanced RNA replication and also secreted more infectious virus (Pietschmann et al., 2006). This indicated that the structural region, p7 or NS2 might influence the efficiency of HCV replication and virus production. Despite multiple efforts (Lindenbach et al., 2005; Pietschmann et al., 2006), it is still not known which regions of the JFH1 genome play a role in its ability to facilitate viral particle secretion, although a recent report found that the JFH1 protease and polymerase are essential for replication of J6/JFH1 recombinants (Murayama et al., 2007). Recently, it was also shown that specific nucleotide changes in the structural region of JFH1 increased virion production (Delgrange et al., 2007). The present work describes the generation of chimeric JFH1 based viruses, with structural and non-structural genes from the HCV strain J6, to optimize virion production. The intragenotypic J6/JFH1 viruses were compared in terms of intracellular replication and infectious virus production and we report here a chimeric virus that robustly produces infectious virus while simultaneously slowing the growth and increasing the number of apoptotic Huh-7.5 transfected cells.

Results

Construction of intragenotypic J6/JFH1 recombinants

Our goal was to better understand the relative contribution of the HCV genome structural and non-structural regions in replication and virion production. Specifically, we studied the effects of exchanging intragenotypic E2, p7, NS2 and NS3 proteins on viral replication and infectivity. To this end, four intragenotypic recombinants were generated in which sequences from the core to part of the protease domain of NS3 protein of the JFH1 clone were replaced with the analogous region derived from HCV J6, also genotype 2a (Yanagi et al., 1999) (Fig. 1A). These recombinants, designated CE2, Cp7, CNS2 and CNS3 comprise J6 genes from core (from amino acid #33) to the C terminal end of E2, p7, NS2, respectively, or to the N-terminal portion of NS3 (including amino acid #79 of NS3). These J6/JFH1 recombinants allowed us to examine the relative contribution of each protein to replication and virus production.

Replication of intragenotypic J6/JFH1 HCV chimeras

In vitro transcribed RNAs were transfected into Huh-7.5 cells, which are highly permissive for HCV replication (Blight et al., 2000). The wild type JFH1 genome and the replication defective mutant genome GND served as positive and negative controls, respectively (Wakita et al., 2005). Replication was monitored at multiple time points after transfection by examining viral protein expression using western blotting for NS3. As shown in Fig. 1B, JFH1 and each of the J6/JFH1 genomes expressed NS3 except, as expected, GND. As observed in Fig. 1B all chimeras showed similar viral protein levels at days 2 and 5 post-transfection, but by day 7 levels of NS3 increased while host cell protein β-actin levels decreased in cells transfected with CE2 and Cp7 clones.

Production of J6/JFH1 chimeric infectious virus

The contribution of the HCV structural proteins to virus assembly and egress is measured by the efficiency of secretion of infectious viral particles. A comparative short and long term quantitative and kinetic analysis of infectious particles released in the supernatant was performed. Viral titers were determined by 50% tissue culture infectivity dose ($TCID_{50}$) at the indicated time points after transfection. The amount of infectious virus released varied among the different J6/JFH1 recombinants when analyzed for 96 hours post-transfection (Fig. 1C). Chimeric viruses Cp7 (4.6 log $TCID_{50}$/ml) and CE2 (4.2 log $TCID_{50}$/ml) showed a 100-fold increase in the amount of infectious virus released in the supernatant when compared to the wild-type JFH1 (1.8 log $TCID_{50}$/ml). Our results confirm the observation that NS2 is important for virus production and release, since the only difference between the Cp7 and CNS2 is that in the Cp7 virus NS2 belongs to the parental JFH1 genome. Moreover, these data show that for each intragenotypic recombinant, J6 structural sequences increase virus release compared to the parental JFH1 clone and that, similar to Pietschmann et al. (2006), virus production can be increased substantially by fusing the pJ6CF structural sequences at or close to the p7-NS2 cleavage site.

Temporal analysis of infectious virion production revealed a decrease in viral titers for each chimera over time (Fig. 1D). For each recombinant, virus production peaked between day 2 and 5 post-transfection with log $TCID_{50}$/mL values of 4.8 for CNS2 and Cp7, 4.5 for CE2, 3.8 for CNS3, and 2.8 for JFH1. JFH1 viral titers decreased rapidly, and were undetectable by day 21. Although the reduction in the level of secreted virus was delayed for CNS2 and CNS3, by day 35 post-transfection no infectious viral particles could be detected in the supernatants of cells transfected with these chimeras. At later time points (day 77) only Cp7 could be detected in the supernatants of Huh-7.5 transfected cells (data not shown).

CE2 and Cp7 recombinant J6/JFH1 viruses are more infectious in vitro

Naive Huh-7.5 cells were infected with the supernatants of cells transfected with the different chimeras to determine whether there were differences in the infectivity of the secreted virus particles. Supernatants of cells transfected with JFH1, GND and the different J6/JFH1 constructs were harvested on day 3 post-transfection. After determining the viral titers, naive Huh-7.5 cells were infected with recombinant virus at a multiplicity of infection (m.o.i.) of 3×10^{-4}. This m.o.i. was chosen to normalize initial infection to JFH1 that showed a maximum viral titer of 2.8 log $TCID_{50}$/ml. At the indicated time points following infection, supernatants were collected for viral titer determination (Fig. 1E). Importantly, viral infectivity determined in four independent low m.o.i. inoculations and measured by $TCID_{50}$/ml was only evident from the CE2 and Cp7 viruses (Fig. 1E), with both establishing a robust infection yielding viral titers of 10^4–10^5 $TCID_{50}$/ml of culture supernatant.

Comparison of infectivity and flexibility of chimeric junctions

Three intragenotypic chimeric viruses expressing the structural region of the pJ6CF clone in the context of JFH1 have been previously described (Lindenbach et al., 2005; Pietschmann et al., 2006). Chimeric virus FL-J6/JFH (Lindenbach et al., 2005) contains part of the 5′ NTR region, core, E1, E2, p7 and NS2 from the pJ6CF clone in the context of the JFH1 genome. For comparison with Cp7 virus, the most efficient of our J6/JFH1 viruses, we constructed an equivalent chimeric virus, NTRNS2. We also constructed a chimeric virus CNS2C3 in which core through the first transmembrane domain of NS2 from JFH1 were replaced by the corresponding region from J6CF. This construct is similar to the J6/C3, and a third construct, CNS2, is similar to the construct J6/C6. Both J6/C3 and J6/C6 were previously reported to be more efficient than JFH1 (Pietschmann et al., 2006). The kinetics of the release of infectious virus by the chimeric viruses Cp7, CNS2, CNS2C3 and NTRNS2, representing all

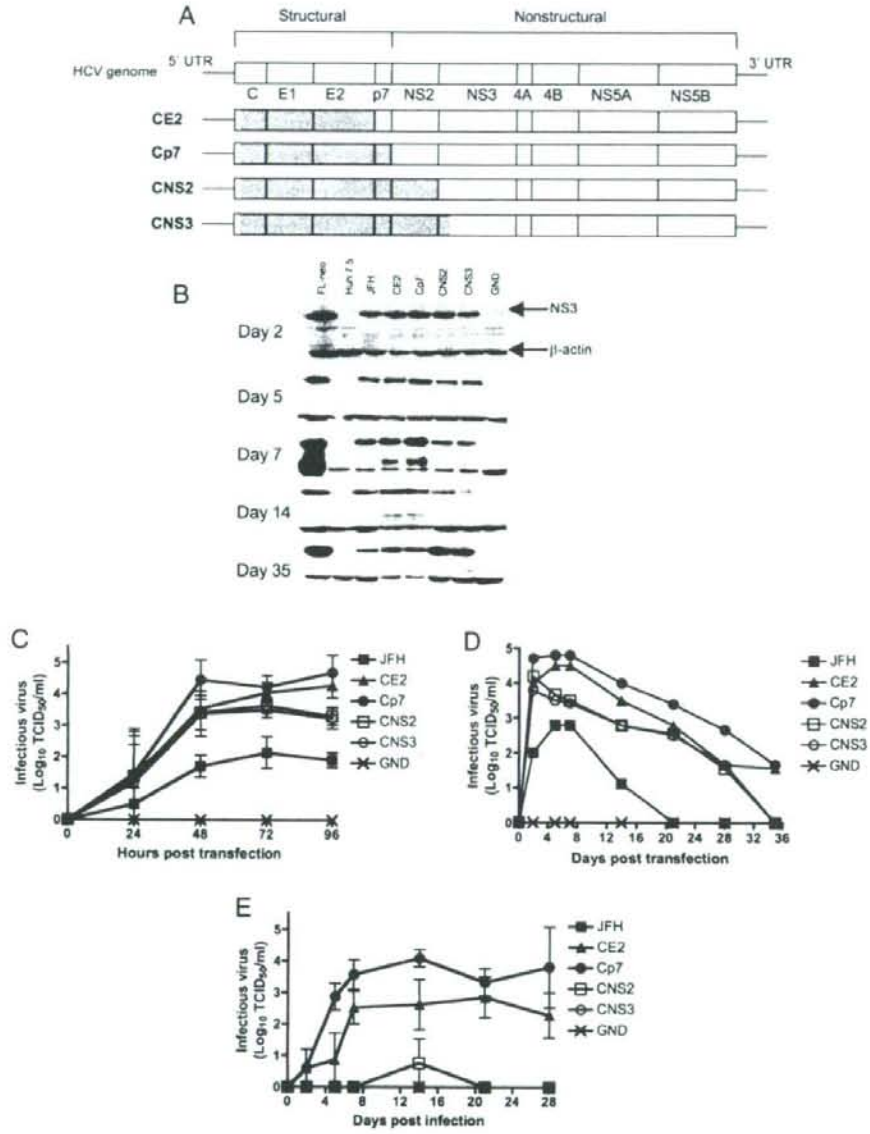

Fig. 1. Replication and protein production of chimeric J6/JFH1 virus. (A) Organization of full-length HCV constructs. Four J6/JFH1 infectious clones were developed by swapping regions from Core to either E2, p7, NS2 or NS3 of the JFH1 genome with the corresponding region of the J6 genome to create CE2, Cp7, CNS2 and CNS3 recombinants, respectively. HCV J6 strain sequences are represented in gray while JFH1 sequences are in white. Ten micrograms of in vitro transcribed RNA were electroporated into 8×10^4 Huh-7.5 cells (B) Intracellular protein production as measured by Western blot analysis. Detection of HCV NS3 antigen in transfected Huh-7.5 cells by Western blot analysis. Cell lysates were prepared and viral and cellular proteins were detected using anti-NS3 monoclonal antibody and anti-β-actin at days 2,5,7,14 and 35 post-transfection. (C) Short term and (D) long term kinetics of chimeric infectious virus particle release in the supernatant ($\log_{10}$ $TCID_{50}$/ml). The data shown in Fig. 1C are a collection of three independent transfections with standard error of mean and 1D is a representative of three independent experiments. Supernatants were harvested at the indicated time points, serially diluted 10-fold and used to inoculate naive Huh-7.5 cells. The viral titers were determined 3 days post infection by immunohistochemistry using monoclonal anti NS5A antibody and by calculating tissue culture infection dose at which 50% of the wells were positive for viral antigen. (E) Kinetics of recombinant chimeric virus infection in naive Huh-7.5 cells. Naive Huh-7.5 cells were inoculated at an m.o.i. of 3×10^{-4} with supernatants of day 3 cultures post-transfection. Infectious virus in the supernatants ($\log_{10}$ $TCID_{50}$/ml) was determined by IHC using anti-NS5A monoclonal antibody at the indicated time points. CNS2, CNS3, GND and JFH showed no infectivity with symbols all overlapping. The data shown in Fig. 1E are a collection of four independent infections with standard error of the mean.

of the intragenotypic chimeras containing the structural genes of J6 reported to date, were compared (Fig. 2A). Supernatants of transfected cells were collected daily for four days and the infectious virus was quantified. As shown in Fig. 2B, the amount of infectious virus secreted in the supernatant of Huh-7.5 cells electroporated with the chimeric RNA transcripts is similar after 24 h post transfection, but after 96 h Cp7 and CNS2C3 are most robustly producing virus. The high titer produced early by Cp7, CNS2C3 and NTRNS2 chimeric viruses indicates that initial

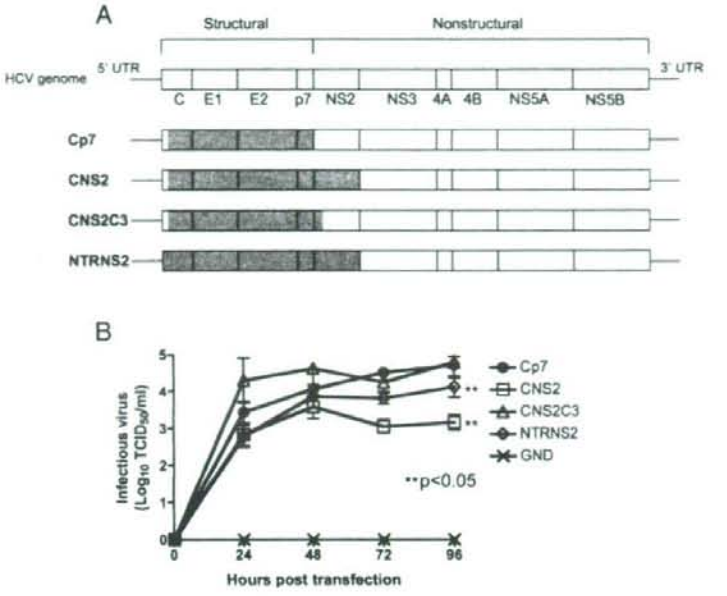

Fig. 2. Virion production by different chimeric constructs. (A) Constructs that are equivalent to the previously reported NTRNS2 and CNS2C3 are shown. (B) In order to compare their ability to produce infectious virions, supernatants were collected and infectivity quantified by IHC assay (log_{10} $TCID_{50}$/ml). Significant differences were observed in levels of infectious virus produced by NTRNS2 and CNS2 96 h post transfection ($p<0.05$). The data shown in Fig. 2B are a collection of at least three independent transfections with standard error of the mean.

infectivity of the chimeric viruses allows some flexibility in the cross over point between pJ6CF and JFH1. In agreement with the results reported by Pietschmann et al. (Pietschmann et al., 2006) CNS2 virus yields were approximately 10-fold lower than CNS2C3 at 72 h post-transfection. This difference became more pronounced (~100-fold) at 96 h post-transfection.

Single mutations in the capsid coding sequence do not affect infectious particles production

Surprisingly, NTRNS2, which is equivalent to FL-J6/JFH reported by Lindenbach et al. (Lindenbach et al., 2005), showed differences after two days post transfection in terms of virion production when compared to CNS2. The differences in sequence between CNS2 and NTRNS2 comprise one nucleotide in the 5′ NTR ($C_{301}U$) and two in the core region: $G_{398}C$ results in an amino acid change ($E_{20}Q$) whereas $C_{412}U$ does not lead to an amino acid change (Fig. 3A). Residue Q_{20} is present in J6 (genotype 2a) as well as in other strains of genotype 1a, 1b, 2f and 2e. Nucleotide position 301 in the 5′ NTR is in domain IIIe of the IRES element of HCV and has been reported to interact with the 40S ribosomal subunit (Spahn et al., 2001) while the other two changes fall in a loop of secondary structure from nucleotide 387 to 424 (McMullan et al., 2007). Both generate changes in the amino acid sequence of the alternative reading frame (ARF) that results from a +1 frameshift (Baril and Brakier-Gingras, 2005). The changes in the ARF are $G_{398}C$ (H →Q) and $C_{412}U$ (S→F). In terms of RNA secondary structure, change $G_{398}C$ is located in a bulge in stem loop V (SLV) and the change $C_{412}U$ disrupts a C–G base pair interaction on SLV (Tuplin et al., 2002) (Fig. 3A). Since it has been previously reported that specific mutations in JFH1 core protein are essential for infectious virus production (Delgrange et al., 2007; Murray et al., 2007), we decided to assess the contribution of these three mutations on initial translation, subsequent replication capacity and virion production. To define the mechanism responsible for the observed difference between CNS2 and NTRNS2 we developed 3 bicistronic genomes (Fig. 3B) in which the 5′ UTR and the first 33 amino acids of core protein are fused with Gaussia luciferase protein (Gluc). In these bicistronic constructs, Gluc is translated from the HCV IRES while in the second cistron, the EMCV IRES initiates the translation of the HCV polyprotein (on the highly efficient Cp7 backbone) at the N-terminus of core. This strategy allows the study of the HCV IRES efficiency independent of replication by determining RLU activity at early time points (Gluc will be generated via translation of the input RNA and subsequently detected and measured in the supernatant) and replication capacity of the genomes by assessing RLU at later time points (replication of the input RNA will continue to generate more Gluc thus leading to an increase as compared to the replication defective GND control). As shown in Fig. 3C, there were no differences in translation efficiencies between CNS2/Gluc/Cp7, NTRNS2/Gluc/Cp7 and the negative control NTR/NS2/Gluc/GND. In terms of replication, both constructs were able to replicate above the levels of the replication defective clone GND (Fig. 3D). To further investigate the effects of these mutations on virion production, we introduced the three individual mutations in the context of the CNS2 monocistronic parental genome. Despite the fact that there were significant differences between CNS2 and NTRNS2 ($p<0.05$), there were not significant differences in terms of virion production 96 h post transfection between the three mutants or the parental CNS2 and NTRNS2 parental clones (Fig. 3E).

Recombinant Cp7 J6/JFH1 virus affects cell division of transfected Huh-7.5 cells

We observed that Huh-7.5 cells transfected with RNA of the Cp7 construct consistently grew slower as compared to cells transfected with JFH or GND. Since Cp7 produced higher viral titers compared with JFH1, we sought to further characterize the effect on host cell growth. Uninfected Huh-7.5 cells were electroporated with in vitro transcribed RNA from JFH1, Cp7 and GND. Measurement of attached

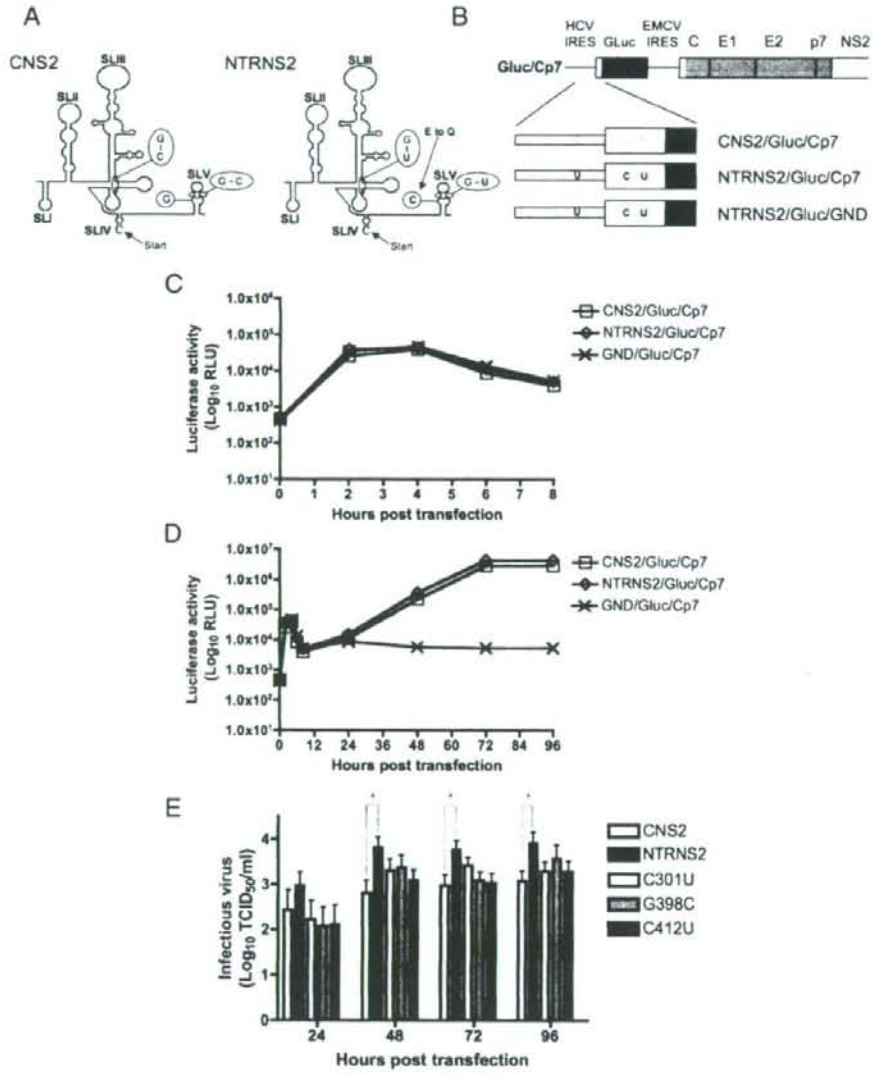

Fig. 3. Single mutations in the capsid coding sequence do not affect infectious particle production. (A) Three nucleotide differences between CNS2 and NTRNS2 J6/JFH1 viruses are shown. The first nucleotide difference is in the IRES element of the 5′ NTR region ($C_{301}U$). In CNS2 there is a G–C pair in stem loop III (SLIII) while in NTRNS2 there is a disruption of this base pairing. The other two differences are in the core protein both in stem loop V (SLV): $G_{398}C$ results in an amino acid change ($E_{20}Q$) whereas $C_{412}U$ does not result in an amino acid change but causes disruption of the Watson–Crick base-pairing. (B) A schematic representation of the full-length bicistronic Gluc reporter plasmids used to analyze the effect of the mutations. The plasmids contain Gluc under the control of the HCV IRES and the Cp7 HCV chimeric genome downstream of EMCV IRES. Bicistronic genomes with mutations in the IRES and core sequence are indicated. (C) Translation and (D) replication of the bicistronic reporter viruses was assessed by transfection of Huh-7.5 cells with 10 μg of in vitro RNA transcribed biscistronic genomes. Supernatants were harvested and assayed by luciferase activity in triplicates (labeled as $\log_{10}$ Relative Luciferase Units, RLU) at the indicated time points post electroporation. The levels of Gaussia luciferase secreted during the first 8 h post transfection are due to translation of the input RNA while the amounts produced 24–96 h post transfection are due to replication of the full-length bicistronic Gluc reporter RNA. (E) Modifications in the 5′ UTR and core coding sequence were engineered in the context of the CNS2 parental virus to compare their capacity to produce infectious virions. Supernatants were harvested and virus quantified infectivity by IHC assay ($\log_{10}$ $TCID_{50}$/ml) at the indicated time points. The data shown in Fig. 3E are a collection of seven independent transfections with standard error of the mean. Amounts of secreted virus in cells transfected with NTRNS2 were significantly higher than CNS2 (asterisks indicate $p<0.05$) 24, 48 and 96 h post transfection.

cell numbers revealed reduced numbers of cells over time in cultures transfected with Cp7 as compared to those transfected with JFH1 or GND (Fig. 4A). To determine whether this difference was secondary to reduced cell division or increased cell death, cells were stained 72 h after transfection with carboxyfluorescein succinimidyl ester (CFSE), which is partitioned equally among daughter cells with each cell division. At the indicated time points, cells were analyzed by flow cytometry. By day 8, cells transfected with Cp7 showed a significantly slower rate of cell division (MFI 595) when compared to those transfected with JFH1 (MFI 172) and GND (MFI 186) (Fig. 4B). These differences remained significant until day 18 after electroporation (Fig. 4C). High intracellular viral replication and virion release may play an important role in the reduced cellular division of Cp7 transfected cells. To confirm that infectious virus was being secreted, viral

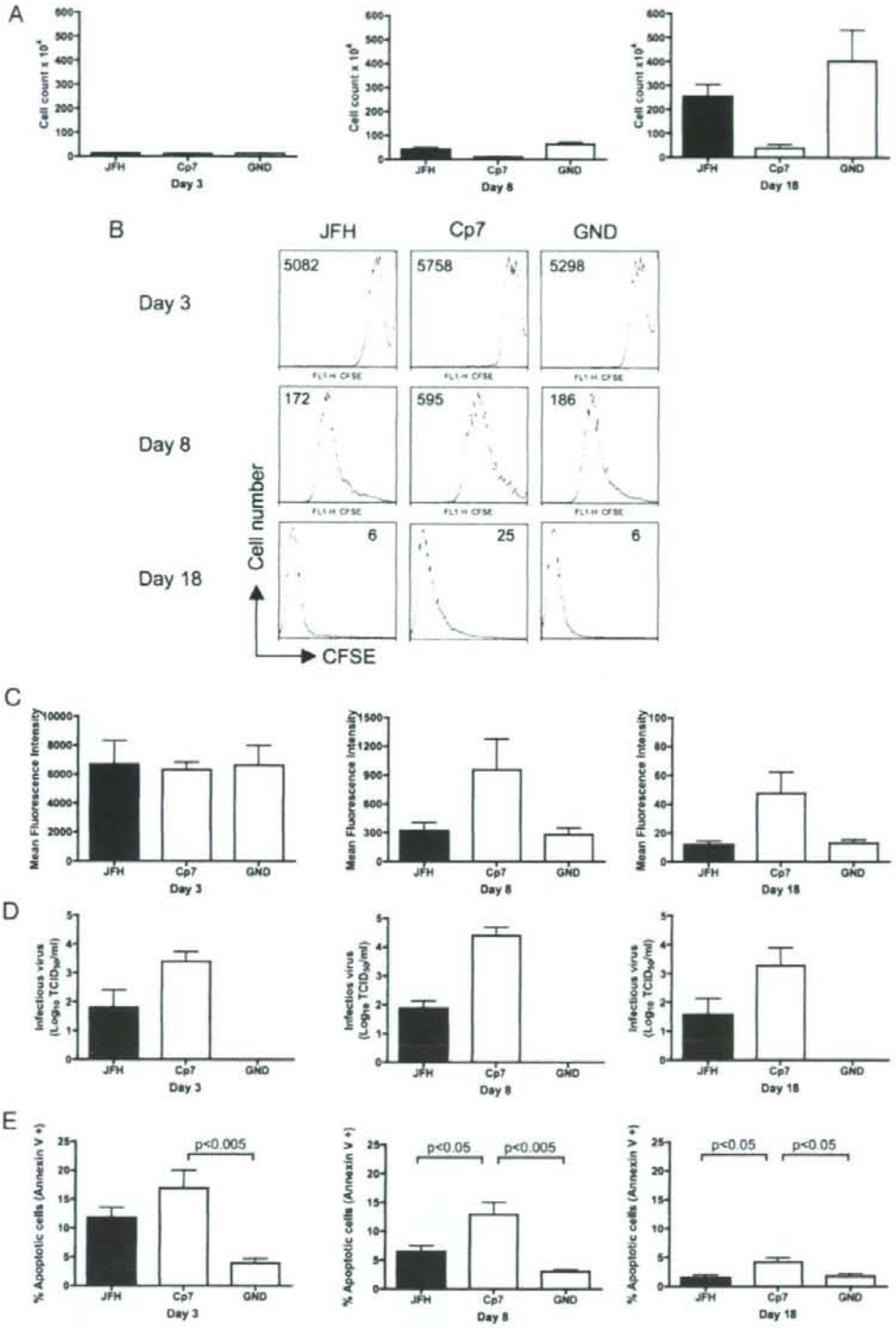
A
Cell count x 10⁴
JFH
Cp7
GND
Day 3
Day 8
Day 18
B
JFH
Cp7
GND
Day 3
Day 8
Day 18
5082
5758
5298
172
595
186
6
25
6
FL1-H CFSE
Cell number
CFSE
C
Mean Fluorescence Intensity
D
Infectious virus (Log10 TCID50/ml)
E
% Apoptotic cells (Annexin V +)
p<0.005
p<0.05
p<0.005
p<0.05
p<0.05

titers were assessed at the indicated time points. More infectious virus was secreted at day 8 in cells transfected with Cp7 (4.1 log $TCID_{50}$/ml) when compared to JFH1 (1.8 log $TCID_{50}$/ml). By day 18, there was a 1.5 log lower titer of virus released by cells transfected with JFH1 as compared to Cp7 (Fig. 4D).

Cp7 replication induces apoptosis in Huh-7.5 cells

The diminution in cell division could be secondary to virus induced cell cycle arrest or apoptosis. The cells transfected with JFH, Cp7 and GND were stained with Annexin-V at days 3, 8 and 18 after electroporation. As shown in Fig. 4E, JFH and Cp7 transfected cells appeared to be undergoing apoptosis as indicated by Annexin V staining at day 3 (11.8% and 16.98% respectively) and day 8 (6.42% and 12.91%, respectively) post transfection. By day 18 only Cp7 transfected cells showed increased percentage of apoptotic cells (4.20%) compared to the background percentage of apoptosis in control GND (1.73%) transfected Huh-7.5 cells. Since the presence of hypodiploid nuclei is an indicator of apoptosis, we additionally used flow cytometric analysis of propidium iodide stained cells and demonstrated that JFH, Cp7 or GND transfected cells were not arrested in a particular phase of cell cycle (data not shown). However we observed that the percentage of hypodiploid cells increased from 7% to almost 20% at day 8 in Cp7 while remaining unchanged for JFH1 and GND transfected cells (data not shown).

Discussion

In this study we described intragenotypic JFH1-based recombinants capable of assembling and releasing infectious viral particles with greater efficiency than the parental JFH1 genome. Through comparison of the known intragenotypic recombinants reported to date, our results confirm previous observations that intragenotypic J6/JFH recombinants including CNS2 of J6 efficiently produce virus (Gottwein et al., 2007; Pietschmann et al., 2006; Yi et al., 2007) but importantly, extend these observations to include more efficient genomes that include only CE2 or Cp7 of J6 and demonstrate decreased cell viability under conditions of high virus production. It is interesting to note that in the study described here, the intracellular accumulation of the NS3 protein (Fig. 1B) was notably greater during the first 14 days after transfection of cells with chimeric CE2 and Cp7, the two constructs that produced the highest levels of infectious virus (Figs. 1C and D), compared to the other chimeras. A recent study by Yi et al. suggests that the intracellular accumulation of core protein correlates closely with virus production (Yi et al., 2007). Although pulse chase studies are required to assess stability of the viral proteins, the authors speculated that the core protein might be stabilized by being packaged into nascent viral particles (Yi et al., 2007).

In our studies of virus release, CE2 and Cp7 robustly secrete infectious virus into the supernatants, followed by CNS2 and CNS3 with similar infectious release kinetics and by JFH1, for which titers are as low as 2 log $TCID_{50}$/ml (Figs. 1C and D). Structural sequences from J6CF increased the efficiency of viral production, as reported by Pietschmann et al. (Pietschmann et al., 2006), indicating that J6 proteins may have a fundamentally better potential for virion assembly and release. As deduced from these results, when NS2 is derived from the same isolate as the nonstructural proteins, the ability to secrete infectious virus into the supernatants is enhanced. Recent studies have additionally reported that when the C-terminal portion of the NS2 is derived from the JFH1 sequence, it is more efficient in producing infectious particles (Pietschmann et al., 2006; Yi et al., 2007). Consistent with replacing JFH1 sequence with J6 sequence, studies of limited mutations in the structural proteins of JFH1 have shown that they actually improve virus production (Delgrange et al., 2007). Furthermore, intergenotypic recombinants acquire compensatory mutations in p7, NS2, NS3, and NS5A that appear to facilitate the release of infectious viral particles (Gottwein et al., 2007; Yi et al., 2007).

In our study, long term kinetic analysis of viral particle release showed a reduction of viral titers with time (Fig. 1D). This reduction may be due to the selection of cells resistant to HCV infection that might have been present in the Huh-7.5 cell line or that emerge during the HCV infection due to the reduction of CD81 expression (Koutsoudakis et al., 2007; Morikawa et al., 2007; Tscherne et al., 2007). Indeed, this phenomenon has previously been observed in Huh-7.5 cells transfected with JFH1 in which levels of secreted virus varied and intracellular HCV RNA levels fluctuated for at least 6 months (Zhong et al., 2006). An important observation is that Cp7 infected cells continued secreting virus during the course of the experiment whereas the levels decreased in Cp7 transfected cells. One possible explanation is that the appearance of resistant cells is perhaps delayed, in cells infected compared to those transfected, since levels of secreted virus peaked at day 7 post-infection whereas the same viral titers (4.5 log $TCID_{50}$/ml for Cp7 and 3.5 log $TCID_{50}$/ml for CE2) are reached at day 2 in transfected cells (Figs. 1C and E). At low m.o.i., only infectivity of CE2 and Cp7 could be recovered confirming the observation that these viruses are more infectious when compared to the other J6/JFH1 chimeras (Fig. 1E). The lack of viral particles released into the supernatants of cells infected with JFH1, CNS2 and CNS3 viruses may be attributed to the conditions of the infection. At very low m.o.i., necessitated by the low titer JFH1, (0.0003 $TCID_{50}$/cell) levels of replication may not be sufficient to produce detectable levels of infectious virus in Huh-7.5 cells and active infection of naive cells is consequently not maintained.

Others have reported the propagation and passage of JFH1 without loss of infectivity in Huh-7.5.1 cells (Zhong et al., 2005, 2006). Zhong et al. reported that JFH1 produced high infectivity titers (10^5–10^6 ffu/ml) within a few days after infection of naive Huh-7.5.1 at an m.o.i. of 0.002 (Zhong et al., 2005) and 0.01 (Zhong et al., 2006). Since Huh-7.5.1 cells were derived from the Huh-7.5 GFP-HCV replicon cell line 1/5A-GFP6 (Moradpour et al., 2004) and were cured with IFN-γ to eliminate the replicon (Zhong et al., 2005), it is possible that Huh-7.5.1 are more amenable to infection with HCV than Huh-7.5 cells. It is however more likely that the high titers were achieved with passaged virus that contained adaptive mutations rather than unmodified JFH1 from transfection supernatant.

The lack of viral particle production from CNS2 infected cells (Fig. 1E) suggests that replacement of JFH NS2 with J6CF sequences is detrimental for virus production at low multiplicity of infection. Previous reports suggest that the most appropriate crossover site in terms of better infectivity is at the transmembrane domain-1 (TMD1) of NS2 (Pietschmann et al., 2006). When we compared J6/C3 (crossover site

Fig. 4. Recombinant virus Cp7 reduces proliferation of Huh-7.5 cells. Cells were electroporated with in vitro transcribed RNA of JFH, Cp7 and GND and were trypsinized and counted at the indicated time points (A). Cells were CFSE labeled two days post transfection. At days 3, 8 and 18 post transfection cells were trypsinized and analyzed by FACS. The columns and bars represent means and standard deviation of four independent transfections. B) Recombinant virus Cp7 retards proliferation of transfected Huh-7.5 cells as demonstrated by the slower rate of CFSE dilution. The numbers in each histogram represent the mean fluorescence intensity (MFI) of the cells at the indicated time points. After one division the MFI decreases geometrically by a factor of two and appears as uniformly spaced clusters on a log scale. (C) MFI of cells transfected with JFH1, Cp7 and GND. Data shown are representative of four separate experiments. (D) Time course of infectious JFH, Cp7 and GND virus released into supernatant ($\log_{10}$ $TCID_{50}$/ml) of RNA transfected and CFSE labeled Huh-7.5 cells. (E) Cp7 induces apoptosis in Huh-7.5 cells as indicated by the increase in the percentage of Annexin-V positive cells. Huh-7.5 transfected with JFH1, Cp7 and GND were trypsinized and stained with Annexin V-APC at days 3, 8 and 18. By day 3 there was a significant increase in the percentage of apoptosis in cells transfected with JFH and Cp7 compared to cells transfected with the GND negative control ($p<0.005$). At day 8 and 18, Cp7 transfected cells showed a significantly higher percentage of apoptotic cells when compared to the parental JFH1 and the GND control ($p<0.005$ and $p<0.05$, respectively). The columns and bars represent means and standard deviation of five independent transfections.

right after the first TMD of NS2) to Cp7 we did not observe a significant difference between Cp7, CNS2C3 and NTRNS2. In agreement with the results reported by Pietschmann et al. (2006), our data show that there is flexibility in the optimal junction for the construction of chimeric HCV genomes in terms of replication efficiency and virus production.

Studies of the 5′ NTR are complicated since the region is known to contain both translation and replication elements (McMullan et al., 2007; Reusken et al., 2003). Recent studies suggest that numerous residues in the core protein are essential for infectious virion production (Murray et al., 2007) possibly due to modulation of host cellular functions. In addition, more robust production of HCV particles can be obtained by introducing a few specific mutations in the core coding sequence of JFH1 (Delgrange et al., 2007). We have performed a comprehensive analysis of the effects on translation and replication of these changes in the core protein in the context of an infectious J6/JFH1 bicistronic reporter virus and subsequently analyzed their impact on virion production by engineering these changes in a monocistronic chimeric virus.

Measuring Gluc activity over time allowed us to assess differences in translation and replication efficiency determined by the three positions that distinguish CNS2 and NTRNS2 (Figs. 3C and D). Since there were no significant differences in translation and replication efficiency between CNS2 and NTRNS2, it is possible that these three mutations may affect packaging and release of viral particles leading to an increase in virion production. Although amino acids 15–28 have been reported to be dispensable for HCV-like particle assembly and morphogenesis (Hourioux et al., 2007), other studies have shown that mutations in the core region might alter RNA packaging, recruitment of nonstructural proteins and replication complexes to lipid droplets, virion assembly and morphogenesis (Boulant et al., 2007; Kim et al., 2006; Miyanari et al., 2007; Rodriguez-Casado et al., 2007) which are critical for the production of infectious virus. We observed a consistent two fold increase in replication levels in NTRNS2 when compared with CNS2, although this difference in replication is not observable in logarithmic scale (Fig. 3D). However, it is possible that slight differences in replication can cause a 10-fold increase in virion production.

When single mutations were engineered in the context if the CNS2 backbone, they did not recapitulate the increased virion production observed for the NTRNS2 clone (Fig. 3E). One possibility is that the combination of mutations is necessary to observe differences in virus production. Core contains conserved RNA structures involved in replication as well as a conserved alternative open reading frame (ARFP) important for HCV replication in vivo and in vitro (McMullan et al., 2007). The C-terminal portion has been implicated in the processing of the core protein from its immature form to the mature form necessary for particle formation (Kato et al., 2003b). Consistent with these data, a recent study by Delgrange et al. showed that two changes in the carboxy terminal region of JFH1 core, implicated in processing core to its mature form, could improve infectious virus production (Delgrange et al., 2007). The authors proposed that these mutations lead to an increase in immature capsid protein (p23) that may be a necessary component for virion production. Interestingly, the E20Q amino acid mutation described in our study (Fig. 3A), in addition to two other mutations described by Kato et al have been identified as important residues conferring increase in p23 levels thus potentially leading to efficient JFH1 particle formation (Kato et al., 2003b).

Interestingly, we observed that the number of Cp7 transfected cells did not increase with the same rate as JFH1 or GND transfected cells (Fig. 4A). To assess if these differences were due to cell death or retardation in cell growth we performed CFSE staining of cells. CFSE staining showed a reduction of cell proliferation in cells transfected with Cp7 (Figs. 4B and C). We could not attribute this phenomenon to cell cycle arrest at any of the distinct phases in the cell cycle, but we observed an increased percentage of apoptosis in cells transfected with JFH1 and Cp7 compared to cells transfected with the GND control (Fig. 4E).

Growth rate was greatly reduced when secreted levels of infectious virus peaked (Fig. 4D). Once the Cp7 extracellular infectious virus levels declined, approximately four weeks post-transfection (Fig. 1D), the effect on cell growth retardation was no longer observed (data not shown). We hypothesize that Cp7 transfected cells grew more slowly and underwent apoptosis (Fig. 4E) because high amounts of virus were secreted. After three weeks, HCV resistant cells or cells that did not secrete high amounts of virus emerged, reducing the levels of secreted virus and allowing increased cell growth. The appearance of HCV resistant cells after infection with JFH1 virus has been previously described and it has been shown to be due to the loss or diminution of CD81 expression in Huh-7.5 and Huh 7 cell lines (Akazawa et al., 2007; Koutsoudakis et al., 2007; Morikawa et al., 2007; Tscherne et al., 2007; Zhong et al., 2006). It is also possible that virus variants could have emerged during the course of the experiment, but this possibility is still under investigation. This raises the interesting question of whether there is an emergence of resistant cells in vivo where viral titers have been reported to be very high.

Although apoptosis plays a central role for the elimination of viral infections there is controversy about whether HCV infection has pro- or anti-apoptotic effects in vivo. There have been reports showing that individual HCV proteins can directly promote or inhibit apoptosis (Nanda et al., 2006; Saito et al., 2006; Szabo, 2006). More recently there have been two reports that have used similar newly developed JFH1 in vitro systems to study viral factors (Sekine-Osajima et al., 2008) and host cell factors (Zhu et al., 2007) affecting apoptosis. In our report, apoptosis of an homogeneous cell population depends on robust virus production. We observed a correlation between particle production, cell growth arrest and apoptosis.

What actually happens in the liver of a patient infected with HCV is not known but it is possible that progressive liver damage might not only be a result of the anti-HCV immune response but also of direct cytopathic effect in virally infected cells. Some indirect evidence for this possibility is that liver injury progresses more rapidly in immune deficient patients than in immune competent HCV infected patients (Thomas and Seeff, 2005). Our established set of intragenotypic chimeras that produce infectious viral particles and in particular, our chimeric virus that comprises sequences from the isolate J6CF from core to p7 in the context of JFH1, will be helpful in examining further the effects of viral mutations, host cell growth retardation and apoptosis, and compensatory changes on infectivity and HCV persistence.

Materials and methods

Cell culture

Huh-7.5 cells (kindly provided by C.M. Rice; (Blight et al., 2002)) were maintained in Dubecco's modified Eagle medium (DMEM) containing 10% heat-inactivated fetal calf serum (Atlanta Biologicals) and incubated at 37 °C, 5% CO_2 and 100% relative humidity.

Construction of full-length chimeric genomes

Plasmids pJFH1 and pGND, full-length genotype 2a cDNA clones, were described previously (Wakita et al., 2005). Plasmid pJ6CF, a full-length clone of HCV genotype 2a, was previously shown to be infectious in chimpanzees (Yanagi et al., 1999).

JFHxJ6 CNS3

Plasmid CNS3 was constructed via 3-piece ligation of the 3222-bp BstZ17I–BbvCI fragment from plasmid pJ6CF, the 6016-bp BbvCI–XbaI fragment and the 3122-bp XbaI–BstZ17I fragment from pJFH1.

JFHxJ6 CE2

To generate plasmid CE2, two PCR products were produced with newly introduced restriction sites to facilitate fusion at the junction of

the E2 gene from pJ6CF and the p7 gene from pJFH1. The first PCR product containing the core-E2 region of pJ6CF was amplified with primer 027HCVC-F (5′-CGTTGGCGGAGTATACTTGT TGCC-3′) and primer 029HCVE2FPCR-R (5′-CTCGCAGCGTGCAAGACGACAAGCT TCTCCAATGCTGCTTCGGCCTGG-3′). The latter introduces a HindIII restriction site (underlined) in the E2–p7 junction. The second PCR product comprised the E2–NS3 region of the JFH1 strain and was amplified using primer 030HCVE2FPRC-F, complementary to 029HCVE2FPCR-R (5′-CCAGGCCGAAGCAGCATTGGAGAAGCTTGTC GTCTTGCACGCTGC-GAG-3′) and 028HCVNS3-R (5′-TACCAAGTCCCCCTCAG CACTCGAGTA-3′). The two products were gel purified and fused via PCR using Vent polymerase (Biolabs) and the primers 027HCVC-F and 028HCVNS3-R. This fusion product was digested with BstZ17I–NotI (2515-bp) and ligated with the 6723-bp NotI–XbaI and 3122-bp XbaI–BstZ17I fragments derived from pJFH1 to generate the full-length clone JFHxJ6 CE2.

JFHxJ6 Cp7

A similar approach was used to construct the full-length clone Cp7. Two PCR products were produced and fused in order to create the junction between the p7 gene from pJ6CF and the NS2 gene from pJFH1. The first PCR product containing the core-p7 region of pJ6CF was amplified with primer 027HCVC-F and primer 031HCVp7FPCR-R (5′-GTCCGTGCACAGGTGCGTCATACGCGTAAGCCTGTTG GGGCAATGC-3′), introducing a MluI restriction site (underlined) in the p7-NS2 junction. The second PCR fragment encoding the NS2 and NS3 genes of pJFH1 was amplified using the primer 032HCVp7FPCR-F (5′-GCATTGC-CCCAACAGGC TTACGCGTATGACGCACCTGT GCACGGAC-3′) that is complementary to 031HCVp7FPCR-R and primer 028HCVNS3-R. Both products were gel purified and fused via PCR using primers 027HCVC-F and 028HCVNS3-R. The resulting fragment was gel purified and digested with BsiWI–NotI (1611-bp) and ligated with the 6723-bp NotI–XbaI fragment derived from pJFH1 and the 4026-bp XbaI–BsiWI fragment derived from JFHxJ6 CNS3 to generate the full-length clone JFHxJ6 Cp7.

JFHxJ6 CNS2

To construct clone CNS2, core-NS2 was amplified from pJ6CF using 035HCVCJ6-F (TCTCGTAGACCGTGCACCATGAGCACAAATCCTAAAC CTCAAAG) and 036HCVCJ6-R (GGCATAAGCAGTGATGGGAGCGAGAA-GACTCCACCCCTTG). To join the NS2 gene from pJ6CF with the NS3 gene from pJFH1, a second PCR product was generated using primers 037HCVNS3JFH-F (GCTCCCATCACTGCTTATGCC) and 038HCVNS3JFH-R (GCTACCGAGGGGTTAAGCACT). Both products were purified and fused via PCR using primers 035HCVCJ6-F and 038HCVNS3JFH-R. This fragment was used in a 3-piece ligation of the 3222-bp BstZ17I–BbvCI fusion PCR product, the 6016-bp BbvCI–XbaI and the 3122-bp XbaI–BstZ17I fragment from pJFH1.

Plasmid CNS2C3 was generated by ligation of the 11,258 bp BsabI–BbvCI fragment derived from the plasmid Cp7 and 1102 pb fusion PCR product digested with the same enzymes. The fusion PCR product was generated by fusing one PCR product generated by amplifying plasmid CNS2 with 027HCV-F and 085JFHJ6NS2C3R 5′-GAGATAGCACAACCACCACAGAAACCGGCTGAGAAGGGTCTT-3′ and a second fragment generated by amplification of pJFH1 plasmid with primers 084JFHJ6NS2C3F 5′-AAGACCCTTCTCAGCCGGTTT-CTGTGGTGGTTGTGCTATCTC-3′ and 028HCVNS3-R. All fragments generated by PCR were verified by sequencing.

Gluc/Cp7and mutant derivatives

Plasmid GLuc/Cp7 was constructed by a three-piece ligation of two fusion PCR products. The first fusion PCR fragment was generated by amplification of two PCR products with primers 060EcoRT7NTRJFH and 136PmelGlucR. The first product (463 bp) was amplified using primers 060EcoRT7NTRJFH (5′-CCGGAATTCTAATACGACTCACTATA-GACC-3′) and 135CoreGLucR (5′-GGGCAAACAGAACTTTGACTCCCATG-TATACTCCGCCA ACGATCT-3′) and JFH1 as a template and encodes from nucleotide 1 to 463 (amino acid 33 of the core protein) of JFH1 plasmid and the first 8 amino acids of *Gaussia* luciferase (GLuc) encoding sequence. The second PCR product used for the fusion was generated by amplification of the sequence encoding for Gluc from plasmid pCMV-Gluc (New England Biolabs) using primers 134CoreGLucF, complementary to 135CoreGLucR (5′-CAGATCGTTGGCGGAGTATACAT-GGGAGTCAAAGTTCTG TTTGCC-3′) and 136PmelGLucR (5′-GTGGTCT-GTTTAAACTTAGTCACCACCGGCCCCCCT-3′) that introduced a PmeI restriction site (underlined) in the 3′ end sequence of Gluc gene. The second fusion PCR product comprised the EMCV IRES sequence fused with the first amino acid of the core protein to part of NS2 from Cp7 and was generated using primers 066EGFPendEMCVSaF and 057HCVNS2JFHR. The EMCV IRES sequence was amplified from the plasmid FL-Neo (kindly provided by CM Rice) using primers 066EGFPendEMCVSaF (5′-GGCATGGACGAGCTCTACAAGTGAGTT-TAAACA GACCACAACGGT-3′) and 067EMCVendCofJFH (GAGGTTTAG-GATTTGTGCTCA TTATTATCGTGTTTTTCAAAGG-3′). The PCR fragment that encodes for the first amino acid of the core protein of JFH1 strain to amino acid 890 in NS2 protein (2668 bp) amplified with primers 068EMCVendCofJFH (5′-CCTTTGAAAAACACGATAATAATGAGCA-CAAATCCTAAACCT-3′) and 057HCVNS2JFHR (5′-AACACCACACCCGGG-CAGAATAT-3′).

To generate the full-length Gluc/Cp7 plasmid, the first product (1115 bp) that encoded for the T7 promoter, HCV IRES and Gluc was digested with EcoRI–PmeI and ligated with the1635 bp-PmeI–BsiWI fragment derived from the second fusion PCR that comprised the EMCV IRES fused with the structural region of Cp7 and a 10992-bp fragment derived from JFH1 digested with EcoRI –BsiWI.

JFH1SphI and mutagenesis

Plasmid JFH1SphI was generated by ligation of 4943-bp fragment generated by digestion of JFH1 with SphI restriction enzyme. The plasmid was used for mutagenesis using QuikChange® XL Site Directed Mutagenesis kit (Stratagene, La Jolla, California). Plasmid C301U JFH1SphI was generated by mutagensis of JFH1SphI with primers 122IRESmutF (5′-GTACTGCCTGATAGGGtGCTTGCGAGTGCCCC-3′) and 123IRESmutR (5′-GGGGCACTCGCAAGCACCCTATCAGGCAGTAC-3′), G398C JFH1SphI with primers 124Core422F (5′-CCAACCGTCGCCCA-CAAGACGTTAAGTTCA-3′) and 125Core422R (5′-TGAACTTAACGT-CTTGTGGGCGACGGTTGG-3′) and C412U JFH1SphI with primers 126Core436F (5′-GAAGACGTTAAGTTtCCGGGCGGCGGCC -3′) and 127Core436R (5′-GGCCGCCGCCCGGAAACTTAACGTCTTC-3′).

NTRNS2/Gluc/Cp7 was obtained by ligation of the EcoRI/PmeI fusion PCR product in which the template for the generation of the first PCR fragment was NTRNS2 plasmid. All constructs were verified by DNA sequencing.

RNA synthesis and transfection

Plasmids containing the full-length chimeric HCV cDNA were linearized by XbaI digestion (Yamazaki et al., 2002) followed by treatment with mung bean nuclease to remove 5′ end overhangs. The linearized DNA templates were purified by phenol:chloroform extraction and ethanol precipitation and resuspended at a final concentration of 1μg/μl. The linearized DNA templates were transcribed with T7 RNA polymerase using a MEGAscript™ T7 kit (Ambion, Austin, TXs) according to the manufacturer. After transcription, synthesized RNA was treated with DNAse I, the integrity of the RNA was analyzed by non-denaturing agarose gel electrophoresis and the yield determined by spectrophotometry and adjusted to 2 μg/μl. RNA was stored at −70 °C until electroporation.

Huh-7.5 cells were grown to 60–80% confluence, trypsinized and washed twice in cold PBS. Cells were resuspended in cold PBS at a concentration of 2×10^7 cells/ml, and 0.4 ml aliquots were mixed with 10 μg of in vitro transcribed RNA and dispensed into 0.4 cm Gene Pulser cuvettes (Bio-Rad). Samples were pulsed using an ECM 830 apparatus

(BTX Genetronics) with five pulses of 99 μsec at 820 V over 1.1 sec. Cells were resuspended in 20 ml of complete growth medium, plated and incubated at 37 °C, 5% CO_2 and 100% relative humidity.

Western blot analysis of HCV proteins

A each time point, cells were washed twice with PBS, lysed with 200 μl of buffer (100 mM Tris, pH 6.8; 20 mM dithiothreitol; 4% (w/v) SDS; 20% glycerol; 0.2% w/v bromophenol blue) and homogenized by passing through a 22-gauge needle. Proteins were separated by SDS-PAGE and transferred to Immobilon-P membranes (Millipore, Bedford, MA). Membranes were blocked with TBS-T (20 mM Tris, pH 7.4, 150 mM NaCl, 0.1% (v/v) Tween-20) with 5% w/v dry milk and HCV proteins were detected using anti-NS3 monoclonal antibody (Virostat), HRP-conjugated secondary antibodies, (Pierce, Rockford, IL) washed repeatedly with TBS-T and detected using an ECL kit (Amersham, NJ).

Viral titration and immnunohistochemical staining

Naive Huh-7.5 cells were grown in collagen coated 96 well plates at a concentration of 6×10^3 cells/well and inoculated with the samples at 10 fold dilutions in 8 replicates at each dilution in complete growth medium. After 3 days of incubation, cells were immunostained for NS5A (Lindenbach et al., 2005). Cell were washed twice with PBS, fixed for 10 min with methanol (−20 °C), washed twice with PBS and permeabilized with one wash of PBS–0.1% Tween 20 (PBS-T). Cells were then blocked for 30 min at room temperature with PBS-T containing 1% (w/v) bovine serum albumin (BSA) and 0.2% dry skim milk, followed by blockage of endogenous peroxidase using 3% H_2O_2 in PBS for 5 min at room temperature. Cells were washed twice with PBS and once with PBS-T and incubated 1 h at room-temperature with a 1:200 dilution of supernatants from the 9E10, anti-NS5A antibody producing, hybridoma (kindly provided by C.M. Rice). After washing twice with PBS and once with PBS-T, cells were incubated with goat anti-mouse HRP polymer (ImmPRESS™-Vector Labs) diluted 1:3 in PBS-T for 30 min at room temperature. Finally, cells were washed as described above and developed using DAB substrate (Vector Laboratories). The viral titers were determined by immunohistochemistry using monoclonal anti NS5A antibody by calculating tissue culture infection dose at which 50% of the wells were positive for viral antigen (Reed and Muench, 1938).

CFSE staining

Seventy-two hours post electroporation supernatants were collected and titered and cells were trypsinized, washed twice with PBS and resuspended at a concentration of $10–15 \times 10^5$ cells/ml. 2 μl of the CFSE stock solution (5 mM in DMSO) were added in 1 ml of PBS and the diluted stock was added to 1 ml of the cell suspension (final concentration of CFSE 5 μM). Cells were labeled for 5 min at room temperature and immediately washed twice with PBS containing 5% FCS. Cells were counted ($3–5 \times 10^5$ cells) and resuspended in 10 ml of MEM with 10% FCS and distributed in 24 well plates.

Supernatants were collected every 48 h and analyzed for viral titers and the cells were trypsinized, counted and analyzed using a FACScalibur cytometer (Becton Dickinson) and FlowJo software (version 6.4).

Annexin APC staining

Apoptosis of transfected Huh-7.5 cells was determined at day 3, 8 and 18 post electroporation by staining with Annexin V-APC (BD Pharmingen™, San Diego, CA) according to the manufacturer's instructions and FACS analysis was carried out on a FACScalibur cytometer. Cells were washed twice with PBS, counted, adjusted to 1×10^6 cells, resuspended in 100 μl of 1X Annexin V binding buffer (10 mM HEPES/NaOH, pH 7.4, 140 mM NaCl, 2.5 mM $CaCl_2$) with 5 μl of Annexin V-APC and incubated for 20 min in the dark. The percentage of apoptotic cells as measured by fluorescence intensity of Annexin V staining was determined using the FACScalibur and FlowJo software (version 6.4).

Acknowledgments

The authors thank Hannah Scarborough and Brian Goldner for their excellent technical assistance and Raghavan Chinnadurai, Tim Denning, Laura McMullan and Holly L. Hanson for their valuable scientific discussion and critical reading of the manuscript. We also thank Charles M. Rice for providing Huh-7.5 and FL-neo cells and the anti-NS5A, clone 9E10/A3 antibody. TW was partially supported by a grant-in-aid for Scientific Research from the Japan Society for the Promotion of Science, from the Ministry of Health, Labor and Welfare of Japan and from the Ministry of Education, Culture, Sports, Science and Technology, and by the Research on Health Sciences Focusing on Drug Innovation from the Japan Health Sciences Foundation. JB was in part supported by grants from the Lundbeck Foundation, the Novo Nordisk Foundation, the Danish Medical Research Council and the A.P. Møller and the Chastine Mc-Kinney Møller Foundation. The authors would like to acknowledge the support from the Cancer Research Institute Investigator Award, Woodruff Health Sciences Fund, EVC/CFAR Flow Cytometry Core P30 AI050409, Yerkes Research Center Base Grant RR-00165, and the public Health Service AI052448 and AI070101(AG).

References

Global surveillance and control of hepatitis C. Report of a WHO Consultation organized in collaboration with the Viral Hepatitis Prevention Board, Antwerp, Belgium. J. Viral Hepatitis 6 (1), 35–47.

Akazawa, D., Date, T., Morikawa, K., Murayama, A., Miyamoto, M., Kaga, M., Barth, H., Baumert, T.F., Dubuisson, J., Wakita, T., 2007. CD81 expression is important for the permissiveness of huh7 cell clones for heterogeneous hepatitis C virus infection. J. Virol. 81 (10), 5036–5045.

Alter, M.J., Margolis, H.S., Krawczynski, K., Judson, F.N., Mares, A., Alexander, W.J., Hu, P.Y., Miller, J.K., Gerber, M.A., Sampliner, R.E., et al., 1992. The natural history of community-acquired hepatitis C in the United States. The Sentinel Counties Chronic non-A, non-B Hepatitis Study Team. N. Engl. J. Med. 327 (27), 1899–1905.

Alter, M.J., Kruszon-Moran, D., Nainan, O.V., McQuillan, G.M., Gao, F., Moyer, L.A., Kaslow, R.A., Margolis, H.S., 1999. The prevalence of hepatitis C virus infection in the United States, 1988 through 1994. N. Engl. J. Med. 341 (8), 556–562.

Baril, M., Brakier-Gingras, L., 2005. Translation of the F protein of hepatitis C virus is initiated at a non-AUG codon in a + 1 reading frame relative to the polyprotein. Nucleic Acids Res. 33 (5), 1474–1486.

Blight, K.J., Kolykhalov, A.A., Rice, C.M., 2000. Efficient initiation of HCV RNA replication in cell culture. Science 290 (5498), 1972–1975.

Blight, K.J., McKeating, J.A., Rice, C.M., 2002. Highly permissive cell lines for subgenomic and genomic hepatitis C virus RNA replication. J. Virol. 76 (24), 13001–13014.

Boulant, S., Targett-Adams, P., McLauchlan, J., 2007. Disrupting the association of hepatitis C virus core protein with lipid droplets correlates with a loss in production of infectious virus. J. Gen. Virol. 88 (Pt 8), 2204–2213.

Bukh, J., Miller, R.H., Purcell, R.H., 1995. Biology and genetic heterogeneity of hepatitis C virus. Clin. Exp. Rheumatol. 13 (Suppl. 13), S3–S7.

Bukh, J., Pietschmann, T., Lohmann, V., Krieger, N., Faulk, K., Engle, R.E., Govindarajan, S., Shapiro, M., St Claire, M., Bartenschlager, R., 2002. Mutations that permit efficient replication of hepatitis C virus RNA in Huh-7 cells prevent productive replication in chimpanzees. Proc. Natl. Acad. Sci. U. S. A. 99 (22), 14416–14421.

Delgrange, D., Pillez, A., Castelain, S., Cocquerel, L., Rouille, Y., Dubuisson, J., Wakita, T., Duverlie, G., Wychowski, C., 2007. Robust production of infectious viral particles in Huh-7 cells by introducing mutations in hepatitis C virus structural proteins. J. Gen. Virol. 88 (Pt 9), 2495–2503.

Gottwein, J.M., Scheel, T.K., Hoegh, A.M., Lademann, J.B., Eugen-Olsen, J., Lisby, G., Bukh, J., 2007. Robust hepatitis C genotype 3a cell culture releasing adapted intergenotypic 3a/2a (S52/JFH1) viruses. Gastroenterology 133 (5), 1614–1626.

Hourioux, C., Ait-Goughoulte, M., Patient, R., Fouquenet, D., Arcanger-Doudet, F., Brand, D., Martin, A., Roingeard, P., 2007. Core protein domains involved in hepatitis C virus-like particle assembly and budding at the endoplasmic reticulum membrane. Cell. Microbiol. 9 (4), 1014–1027.

Kato, T., Furusaka, A., Miyamoto, M., Date, T., Yasui, K., Hiramoto, J., Nagayama, K., Tanaka, T., Wakita, T., 2001. Sequence analysis of hepatitis C virus isolated from a fulminant hepatitis patient. J. Med. Virol. 64 (3), 334–339.

Kato, T., Date, T., Miyamoto, M., Furusaka, A., Tokushige, K., Mizokami, M., Wakita, T., 2003a. Efficient replication of the genotype 2a hepatitis C virus subgenomic replicon. Gastroenterology 125 (6), 1808–1817.

Kato, T., Miyamoto, M., Furusaka, A., Date, T., Yasui, K., Kato, J., Matsushima, S., Komatsu, T., Wakita, T., 2003b. Processing of hepatitis C virus core protein is regulated by its C-terminal sequence. J. Med. Virol. 69 (3), 357–366.

Kim, M., Ha, Y., Park, H.J., 2006. Structural requirements for assembly and homotypic interactions of the hepatitis C virus core protein. Virus Res. 122 (1–2), 137–143.
Koutsoudakis, G., Herrmann, E., Kallis, S., Bartenschlager, R., Pietschmann, T., 2007. The level of CD81 cell surface expression is a key determinant for productive entry of hepatitis C virus into host cells. J. Virol. 81 (2), 588–598.
Lindenbach, B.D., Rice, C.M., 2005. Unravelling hepatitis C virus replication from genome to function. Nature 436 (7053), 933–938.
Lindenbach, B.D., Evans, M.J., Syder, A.J., Wolk, B., Tellinghuisen, T.L., Liu, C.C., Maruyama, T., Hynes, R.O., Burton, D.R., McKeating, J.A., Rice, C.M., 2005. Complete replication of hepatitis C virus in cell culture. Science 309 (5734), 623–626.
Lohmann, V., Korner, F., Koch, J., Herian, U., Theilmann, L., Bartenschlager, R., 1999. Replication of subgenomic hepatitis C virus RNAs in a hepatoma cell line. Science 285 (5424), 110–113.
McMullan, L.K., Grakoui, A., Evans, M.J., Mihalik, K., Puig, M., Branch, A.D., Feinstone, S.M., Rice, C.M., 2007. Evidence for a functional RNA element in the hepatitis C virus core gene. Proc. Natl. Acad. Sci. U. S. A. 104 (8), 2879–2884.
Miyanari, Y., Atsuzawa, K., Usuda, N., Watashi, K., Hishiki, T., Zayas, M., Bartenschlager, R., Wakita, T., Hijikata, M., Shimotohno, K., 2007. The lipid droplet is an important organelle for hepatitis C virus production. Nat. Cell Biol. 9 (9), 1089–1097.
Moradpour, D., Evans, M.J., Gosert, R., Yuan, Z., Blum, H.E., Goff, S.P., Lindenbach, B.D., Rice, C.M., 2004. Insertion of green fluorescent protein into nonstructural protein 5A allows direct visualization of functional hepatitis C virus replication complexes. J. Virol. 78 (14), 7400–7409.
Moradpour, D., Penin, F., Rice, C.M., 2007. Replication of hepatitis C virus. Nat. Rev., Microbiol. 5 (6), 453–463.
Morikawa, K., Zhao, Z., Date, T., Miyamoto, M., Murayama, A., Akazawa, D., Tanabe, J., Sone, S., Wakita, T., 2007. The roles of CD81 and glycosaminoglycans in the adsorption and uptake of infectious HCV particles. J. Med. Virol. 79 (6), 714–723.
Murayama, A., Date, T., Morikawa, K., Akazawa, D., Miyamoto, M., Kaga, M., Ishii, K., Suzuki, T., Kato, T., Mizokami, M., Wakita, T., 2007. The NS3 helicase and NS5B-to-3'X regions are important for efficient hepatitis C virus strain JFH-1 replication in Huh7 cells. J. Virol. 81 (15), 8030–8040.
Murray, C.L., Jones, C.T., Tassello, J., Rice, C.M., 2007. Alanine scanning of the hepatitis C virus core protein reveals numerous residues essential for production of infectious virus. J. Virol. 81 (19), 10220–10231.
Nanda, S.K., Herion, D., Liang, T.J., 2006. The SH3 binding motif of HCV [corrected] NS5A protein interacts with Bin1 and is important for apoptosis and infectivity. Gastroenterology 130 (3), 794–809.
Pietschmann, T., Kaul, A., Koutsoudakis, G., Shavinskaya, A., Kallis, S., Steinmann, E., Abid, K., Negro, F., Dreux, M., Cosset, F.L., Bartenschlager, R., 2006. Construction and characterization of infectious intragenotypic and intergenotypic hepatitis C virus chimeras. Proc. Natl. Acad. Sci. U. S. A. 103 (19), 7408–7413.
Reed, L.J., Muench, H., 1938. A simple method of estimating fifty percent endpoints. Am. J. Hyg. 27 (3), 493–497.
Reichard, O., Schvarcz, R., Weiland, O., 1997. Therapy of hepatitis C: alpha interferon and ribavirin. Hepatology 26, 108S–111S.
Reusken, C.B., Dalebout, T.J., Eerligh, P., Bredenbeek, P.J., Spaan, W.J., 2003. Analysis of hepatitis C virus/classical swine fever virus chimeric 5' NTRs: sequences within the hepatitis C virus IRES are required for viral RNA replication. J. Gen. Virol. 84 (Pt 7), 1761–1769.
Rodriguez-Casado, A., Molina, M., Carmona, P., 2007. Core protein-nucleic acid interactions in hepatitis C virus as revealed by Raman and circular dichroism spectroscopy. Appl. Spectrosc. 61 (11), 1219–1224.
Saito, K., Meyer, K., Warner, R., Basu, A., Ray, R.B., Ray, R., 2006. Hepatitis C virus core protein inhibits tumor necrosis factor alpha-mediated apoptosis by a protective effect involving cellular FLICE inhibitory protein. J. Virol. 80 (9), 4372–4379.
Sakai, A., Takikawa, S., Thimme, R., Meunier, J.C., Spangenberg, H.C., Govindarajan, S., Farci, P., Emerson, S.U., Chisari, F.V., Purcell, R.H., Bukh, J., 2007. In vivo study of the HC-TN strain of hepatitis C virus recovered from a patient with fulminant hepatitis: RNA transcripts of a molecular clone (pHC-TN) are infectious in chimpanzees but not in Huh7.5 cells. J. Virol. 81 (13), 7208–7219.
Sekine-Osajima, Y., Sakamoto, N., Mishima, K., Nakagawa, M., Itsui, Y., Tasaka, M., Nishimura-Sakurai, Y., Chen, C.H., Kanai, T., Tsuchiya, K., Wakita, T., Enomoto, N., Watanabe, M., 2008. Development of plaque assays for hepatitis C virus-JFH1 strain and isolation of mutants with enhanced cytopathogenicity and replication capacity. Virology 371 (1), 71–85.
Spahn, C.M., Kieft, J.S., Grassucci, R.A., Penczek, P.A., Zhou, K., Doudna, J.A., Frank, J., 2001. Hepatitis C virus IRES RNA-induced changes in the conformation of the 40s ribosomal subunit. Science 291 (5510), 1959–1962.
Szabo, G., 2006. Hepatitis C virus NS5A protein—a master regulator? Gastroenterology 130 (3), 995–999.
Thomas, D.L., Seeff, L.B., 2005. Natural history of hepatitis C. Clin. Liver Dis. 9 (3), 383–398 vi.
Tscherne, D.M., Evans, M.J., von Hahn, T., Jones, C.T., Stamataki, Z., McKeating, J.A., Lindenbach, B.D., Rice, C.M., 2007. Superinfection exclusion in cells infected with hepatitis C virus. J. Virol. 81 (8), 3693–3703.
Tuplin, A., Wood, J., Evans, D.J., Patel, A.H., Simmonds, P., 2002. Thermodynamic and phylogenetic prediction of RNA secondary structures in the coding region of hepatitis C virus. RNA 8 (6), 824–841.
Wakita, T., Pietschmann, T., Kato, T., Date, T., Miyamoto, M., Zhao, Z., Murthy, K., Habermann, A., Krausslich, H.G., Mizokami, M., Bartenschlager, R., Liang, T.J., 2005. Production of infectious hepatitis C virus in tissue culture from a cloned viral genome. Nat. Med. 11 (7), 791–796.
Wasley, A., Alter, M.J., 2000. Epidemiology of hepatitis C: geographic differences and temporal trends. Semin. Liver Dis. 20 (1), 1–16.
Yamazaki, T., Akiba, H., Iwai, H., Matsuda, H., Aoki, M., Tanno, Y., Shin, T., Tsuchiya, H., Pardoll, D.M., Okumura, K., Azuma, M., Yagita, H., 2002. Expression of programmed death 1 ligands by murine T cells and APC. J. Immunol. 169 (10), 5538–5545.
Yanagi, M., Purcell, R.H., Emerson, S.U., Bukh, J., 1999. Hepatitis C virus: an infectious molecular clone of a second major genotype (2a) and lack of viability of intertypic 1a and 2a chimeras. Virology 262 (1), 250–263.
Yi, M., Ma, Y., Yates, J., Lemon, S.M., 2007. Compensatory mutations in E1, p7, NS2, and NS3 enhance yields of cell culture-infectious intergenotypic chimeric hepatitis C virus. J. Virol. 81 (2), 629–638.
Zhong, J., Gastaminza, P., Cheng, G., Kapadia, S., Kato, T., Burton, D.R., Wieland, S.F., Uprichard, S.L., Wakita, T., Chisari, F.V., 2005. Robust hepatitis C virus infection in vitro. Proc. Natl. Acad. Sci. U. S. A. 102 (26), 9294–9299.
Zhong, J., Gastaminza, P., Chung, J., Stamataki, Z., Isogawa, M., Cheng, G., McKeating, J.A., Chisari, F.V., 2006. Persistent hepatitis C virus infection in vitro: coevolution of virus and host. J. Virol. 80 (22), 11082–11093.
Zhu, H., Dong, H., Eksioglu, E., Hemming, A., Cao, M., Crawford, J.M., Nelson, D.R., Liu, C., 2007. Hepatitis C virus triggers apoptosis of a newly developed hepatoma cell line through antiviral defense system. Gastroenterology 133 (5), 1649–1659.

Journal of Medical Virology 80:980–988 (2008)

Impaired Cytokine Response in Myeloid Dendritic Cells in Chronic Hepatitis C Virus Infection Regardless of Enhanced Expression of Toll-Like Receptors and Retinoic Acid Inducible Gene-I

Masanori Miyazaki,[1] Tatsuya Kanto,[1,2] Michiyo Inoue,[2] Ichiyo Itose,[1] Hideki Miyatake,[1] Mitsuru Sakakibara,[1] Takayuki Yakushijin,[1] Naruyasu Kakita,[1] Naoki Hiramatsu,[1] Tetsuo Takehara,[1] Akinori Kasahara,[3] and Norio Hayashi[1]*

[1]*Department of Gastroenterology and Hepatology, Osaka University Graduate School of Medicine, Osaka, Japan*
[2]*Department of Dendritic Cell Biology and Clinical Application, Osaka University Graduate School of Medicine, Osaka, Japan*
[3]*Department of General Medicine, Osaka University Graduate School of Medicine, Osaka, Japan*

Dendritic cells utilize various sets of Toll-like receptors (TLR) or cytosolic sensors to detect pathogens and evoke immune responses. In patients with hepatitis C virus (HCV) infection, a higher prevalence of various infectious diseases is reported; suggesting that innate immunity against pathogens is impaired. The aim of this study was to clarify whether the TLR and retinoic acid inducible gene-I (RIG-I) system in myeloid dendritic cells is preserved or not in chronic HCV infection. The expression of TLRs, RIG-I and its relatives were compared in myeloid dendritic cells between 39 patients and 52 healthy volunteers. The induction of type-I interferon (IFN) and inflammatory cytokines was examined in response to agonists for TLR2 (palmitoyl-3-cysteine-serine-lysine-4), TLR3/RIG-I (polyinosine–polycytidylic acid) or TLR4 (lipopolysaccharide). The relative expressions of TLR2, TLR4, RIG-I, and LGP2 from the patients were significantly higher than those from the volunteers, whereas TLR3 and MDA-5 expressions did not differ. In search for factors regulating TLR/RIG-I expression, it was shown that IFN-α, polyinosine–polycytidylic acid and lipopolysaccharide induced TLR3, TLR4 and RIG-I, but TNF-α, HCV core or HCV non-structural proteins did not. For the functional analyses, myeloid dendritic cells from the patients induced significantly less amounts of IFN-β, TNF-α and IL-12p70 in response to polyinosine–polycytidylic acid or lipopolysaccharide. It is noteworthy that the expression of TRIF and TRAF6, which are essential adaptor molecules transmitting TLR3 or TLR4-dependent signals, is reduced in the patients. Thus, innate cytokine responses in myeloid dendritic cells are impaired regardless of enhanced expressions of TLR2, TLR4, and RIG-I in HCV infection. ***J. Med. Virol. 80: 980–988, 2008.*** © 2008 Wiley-Liss, Inc.

KEY WORDS: chronic hepatitis C; myeloid dendritic cell; innate immunity; TLR3; RIG-I

INTRODUCTION

Hepatitis C virus (HCV) is a single-stranded RNA virus, which causes chronic liver disease in hosts. At primary HCV infection, approximately 80% of patients fail to eradicate HCV and eventually progress to a chronic infected state [Lauer and Walker, 2001]. It is very likely that escape mutation of the HCV genome and insufficient immune responses against HCV in hosts are involved in the persistence of infection, however, the precise mechanisms are still largely unknown. Type-I interferon (IFN) is a potent anti-viral agent that exerts its ability by suppressing viral replication or via modulating immune reactions. Gene expression analyses of HCV-infected livers obtained from chimpanzees revealed that type-I IFN and IFN-stimulated genes are highly induced even in the incubation phase [Bigger et al., 2004]. Nevertheless, HCV continues to replicate and remains at high titer levels, suggesting that HCV

Grant sponsor: Ministry of Education, Culture, Sports, Science and Technology; Grant sponsor: Ministry of Health, Labor and Welfare of Japan.

*Correspondence to: Norio Hayashi, MD, PhD, Department of Gastroenterology and Hepatology, Osaka University Graduate School of Medicine, 2-2 Yamada-oka, Suita, Osaka 565-0871, Japan. E-mail: hayashin@gh.med.osaka-u.ac.jp

Accepted 5 February 2008

DOI 10.1002/jmv.21174

Published online in Wiley InterScience (www.interscience.wiley.com)

possesses some inhibitory mechanisms in IFN-inducible anti-viral responses.

As for the mechanisms of HCV persistence, the alteration or impairment of various immune cells has been reported, such as T cells, NK cells and dendritic cells [Chang et al., 2001; Wedemeyer et al., 2002; Kanto et al., 2004; Szabo and Dolganiuc, 2005]. In clear contrast with the human immunodeficiency virus, HCV does not lead to generalized immune suppression in infected hosts. Large-scale epidemiological study on US veterans revealed that the prevalence of various infectious diseases was significantly higher in HCV-positive individuals than in HCV-negative ones, including viral, bacterial, and parasite diseases [El-Serag et al., 2003]. These observations suggest that HCV infection raises the susceptibility to pathogens, not profoundly but significantly, in infected patients. However, the underlying mechanisms in the increased prevalence of infection are yet to be determined.

Toll-like receptors (TLR) are expressed in epithelial cells or antigen presenting cells and act as sensors of bacterial or viral infection. These cells utilize specific TLR for the recognition of pathogen-associated molecular patterns and eventually induce type I IFN or inflammatory cytokines. In addition to the TLR system, the existence of cytoplasmic receptors for dsRNA has been reported as virus sensors, which are retinoic acid inducible protein I (RIG-I) and melanoma differentiation associated gene 5 (MDA-5) [Yoneyama et al., 2004]. Since dsRNA is a replicative intermediate of RNA virus, RIG-I and MDA-5 induce IFN-β in response to virus infection independently of TLR3. It is thus plausible that a disabled TLR/RIG-I system may be involved in the increased susceptibility to pathogens or the mechanisms of persistent virus infection [Sumpter et al., 2005]. In human hepatoma cells harboring HCV replicons, it has been shown that HCV NS3/4A protease impedes TLR3-dependent or RIG-I-dependent IFN-β induction by means of the cleavage of relevant adaptor molecules, such as TIR domain-containing adapter inducing IFN-β (TRIF) or interferon-β promoter stimulator-1 (IPS-1), respectively [Foy et al., 2005; Li et al., 2005]. However, it is not clear whether similar inhibitory machinery of HCV operates or not in immune cells, such as dendritic cells.

Dendritic cells are immune sentinels that play a central role against pathogens in inducing innate as well as adaptive immune responses. Dendritic cells consist of myeloid and plasmacytoid subsets that play distinct roles in the regulation of immune responses. Dendritic cells utilize various sets of TLR or RIG-I/MDA-5 to sense virus infection. After the recognition, dendritic cells begin to mature and gain the ability to produce type-I IFN and inflammatory cytokines. It has been reported that blood dendritic cells expresses distinct profiles of TLRs; human myeloid dendritic cells express TLR2, -3, -4, -5, -6, -7, and -8, while plasmacytoid dendritic cells express TLR7, -8 and -9 [Iwasaki and Medzhitov, 2004]. Numerical and/or functional impairment of blood dendritic cells in acute or chronic HCV infection has been reported by several investigators including us [Kanto et al., 2004; Szabo and Dolganiuc, 2005]. One of the plausible mechanisms leading to dendritic cells impairment may be direct HCV infection to blood dendritic cells or their precursors. In support for this, it was shown that myeloid dendritic cells are susceptible to HCV infection, judging from the results of an inoculation study with pseudo-HCV particles or detection of negative strand HCV-RNA [Kaimori et al., 2004]. According to another report, myeloid dendritic cells displayed impaired expression of IL-12 and TNF-α in response to polyinosine–polycytidylic acid (polyI:C) and lipopolysaccharide (LPS) in patients with a large amount of cell-associated HCV [Rodrigue-Gervais et al., 2007], suggesting a possible link between direct HCV infection to myeloid dendritic cells and an impaired innate response.

Taking these reports into consideration, the current study focused on myeloid dendritic cells in order to clarify the roles of the TLR/RIG-I system in HCV infection, by comparing the expression of TLR, RIG-I, and MDA-5 and the induction of cytokines in response to specific agonists for these virus sensors. The study demonstrated that myeloid dendritic cells from HCV-infected patients induces a significantly lesser amount of cytokines in spite of enhanced expressions of TLR2, TLR4, and RIG-I. These findings imply that alteration of the TLR/RIG-I system is instrumental in impairment of innate immunity in HCV infection, where myeloid dendritic cells play a key role as immune sentinels against pathogens.

MATERIALS AND METHODS

Subjects

Thirty-nine patients (male/female: 22/17, mean age: 53.4 ± 10.3 years old, mean serum ALT levels: 93.9 ± 51.0 IU/L, HCV serotype 1/serotype 2: 39/0) with chronic hepatitis C (HCV group) followed at Osaka University Hospital (Osaka, Japan) were enrolled in the present study. All of them were confirmed to be positive for both serum anti-HCV antibody and HCV RNA (mean HCV RNA quantity assayed by Cobas Amplicor HCV monitor v 2.0, Roche Diagnostics, Tokyo, Japan; [Pawlotsky et al., 2000]: 1,637 ± 402 KIU/ml) but were negative for other viral infections, including hepatitis B virus (HBV) and human immunodeficiency virus (HIV). The presence of other liver diseases, such as alcoholic, metabolic or autoimmune hepatitis, was ruled out. Thirteen patients with chronic HBV infection determined by serum HBsAg-positive and ALT abnormality (male/female: 6/7, HBeAg+/HBeAg−: 7/6, mean age: 45.9 ± 14.4 years old, mean serum ALT levels: 95.2 ± 145 IU/L, mean HBV-DNA levels assayed by Cobas Amplicor HBV monitor Roche Diagnostics; [Noborg et al., 1999]: 6.1 ± 1.7 $\log_{10}$ copies/ml) were also enrolled as disease controls (HBV group). The study protocol was approved by the ethical committee of Osaka University Graduate School of Medicine. At enrolment, written informed consent was obtained from each patient. The

controls were 52 healthy volunteers or blood donors (healthy donors group) at the Osaka Red Cross Blood Center (Osaka, Japan), who were confirmed to be negative for HCV, HBV, and HIV. The background data of the blood donors were not accessible due to the confidentiality regulations of the blood center, but their serum ALT levels were confirmed to be within the normal range.

Reagents

Palmitoyl-3-cysteine-serine-lysine-4 (Pam_3CSK_4) was purchased from InvivoGen (San Diego, CA). Polyinosine–polycytidylic acid (polyI:C) and lipopolysaccharide (LPS) from *Escherichia coli* were purchased from Sigma (St. Louis, MO). Recombinant human IL-6, IL-10, and IL-12 were purchased from InvivoGen. Recombinant TNF-α was purchased from Genzyme (Framingham, MA). Recombinant HCV structural or non-structural (NS) proteins expressed by *E. coli* were purchased from Virogen (Watertown, MA). They were HCV core (amino acid positions, from 2 to 192), NS3 (from 1,450 to 1,643), and NS4 (from 1,658 to 1,863), respectively. HCV NS5B protein (from 2,421 to 2,965) was kindly provided by Japan Tobacco Corp. (Tokyo, Japan). Natural human interferon-α was purchased from Otsuka Pharmaceutical Co. (Tokyo, Japan).

Isolation of Myeloid Dendritic Cells

Peripheral blood mononuclear cells were isolated from heparinized venous blood by centrifugation on Ficoll-Hypaque cushion as described previously [Kanto et al., 2004]. Myeloid dendritic cells were magnetically isolated using a BDCA-1 Isolation Kit (Miltenyi Biotec, Auburn, CA) according to the manufacturer's instructions. The purity of myeloid dendritic cells (Lineage-negative, $HLA\text{-}DR^+$, $CD11c^+$, and $CD123^{dim+}$ cells) was more than 95% as assessed by FACS (data not shown). Short-term culture of myeloid dendritic cells was performed in cytokine-free Isocove's modified Dulbecco's medium (GIBCO Laboratories, Grand Island, NY) supplemented with 10% fetal calf serum, 100 μg/mL streptomycin, 100 U/mL penicillin, 2 mmol/L L-glutamine, 5 mmol/L HEPES, and 5 mmol/L non-essential amino acid at 37°C in 5% CO_2.

To clarify the factors influencing the expressions of TLR or RIG-I in myeloid dendritic cells, fresh myeloid dendritic cells obtained from uninfected controls were incubated for 2 hr in the presence or absence of various cytokines, agonists for TLR/RIG-I or recombinant HCV proteins. After the incubation, they were subjected to RT-PCR analyses for the comparison.

In order to compare the function of TLR/RIG-I-mediated responses in myeloid dendritic cells between the groups, myeloid dendritic cells were incubated with various agonists for 2 hr and subjected them to cytokine analysis by RT-PCR. Alternatively, myeloid dendritic cells were cultured in the presence or absence of 25 μg/ml of polyI:C for 24 hr and collected supernatants for subsequent cytokine analyses.

Flowcytometric Analysis

The phenotypes of myeloid dendritic cells were analyzed using FACS Calibur and CellQuest software (BD Biosciences, San Jose, CA). For the staining, myeloid dendritic cells were incubated with specific antibodies for 15 min at room temperature in phosphate buffered saline (PBS) containing 2% of bovine serum albumin and 0.1% of sodium azide. The following FITC-, PE-, or APC-conjugated anti-human monoclonal antibodies were used: CD11c (clone, B-ly6), HLA-DR (L243), CD80 (L307.4), CD86 (IT2.2), CD40 (5C3), and CD83 (HB15e). All were purchased from BD Biosciences.

Real-Time Quantitative PCR

Total RNA was extracted from more than 10^6 myeloid dendritic cells using RNeasy Mini kit (Qiagen, Hilden, Germany), which was subsequently reverse transcribed in 20 μl volume using SuperScript III First-Strand Synthesis System (Invitrogen Corp., Carlsbad, CA) according to the manufacturer's instructions. Random hexamers were added as primers. The mRNA levels were evaluated using ABI PRISM 7900 Sequence Detection System (Applied Biosystems, Foster City, CA). For the quantification of TLR2, TLR3, TLR4, RIG-I, MDA-5, LGP2, myeloid differentiation factor 88 (MyD88), IPS-1, TRIF, TNF receptor associated factor 6 (TRAF6), TNF-α and IFN-β, ready-to-use assays (Taqman Gene Expression Assays, Applied Biosystems) were utilized, according to the manufacturer's instructions. All of the reagents used for PCR were purchased from Applied Biosystems. All of the reactions were performed in duplicate. The thermal cycling conditions for all genes were 2 min at 50°C and 10 min at 95°C, followed by 40 cycles at 95°C for 15 sec and 60°C for 1 min. A calibrator sample from healthy volunteers was identified. The expressions of molecule were expressed as the relative values to the calibrator samples. To standardize the amount of total RNA added to each reaction mixture, β-actin mRNA from each sample was quantified as a control of internal RNA and corrected all values with this.

Enzyme-Linked Immunosorbent Assay and Cytokine Beads Assay

The quantity of IFN-α in culture supernatants was evaluated using Human Interferon Alpha ELISA kit (PBL Biomedical Laboratories, New Brunswick, NJ) according to the manufacturer's instructions. The concentration of TNF-α, IL-6, and IL-12p70 in the supernatants was assayed by the use of BD cytokine beads assay (CBA) Flex Sets (BD Biosciences) and analyzed by FACS Calibur according to the manufacture's instructions. The detection limits of IFN-α, TNF-α, IL-6, and IL-12p70 are 10–5,000 pg/ml, respectively.

Statistical Analysis

The Mann–Whitney *U*-test was performed to evaluate differences among the groups using StatView

5.0 software (SAS Institute, Cary, NC). A P-value of <0.05 was considered to be statistically significant.

RESULTS

Expressions of TLR2, TLR4, and RIG-I Were Higher in Myeloid Dendritic Cells From Chronic Hepatitis C Patients

With respect to the phenotypes of fresh myeloid dendritic cells, the expressions of maturation markers such as CD40, CD80, CD83, and CD86 were relatively low and were not different between the HCV group and healthy donor group (Fig. 1). The similar results were obtained from HBV group (data not shown). These results show that myeloid dendritic cells from all groups are equally immature phenotypes.

First, the expressions of TLR2, TLR3, and TLR4 in myeloid dendritic cells were examined. The relative amounts of TLR2 and TLR4 in the HCV group were higher than those in healthy donors or the HBV group (Fig. 2). In contrast, the TLR3 expression was not different among the groups (Fig. 2). In comparison between HBV and healthy donor groups, there was no difference in the expressions of these TLRs in myeloid dendritic cells (Fig. 2).

The expression of cytoplasmic receptors for dsRNA in myeloid dendritic cells was also compared. The RIG-I and LGP2 expression in the HCV or the HBV group was significantly higher than those from healthy donors, whereas MDA-5 did not differ among the groups (Fig. 2). No correlation was found among the expressions of any TLR and dsRNA receptors (data not shown).

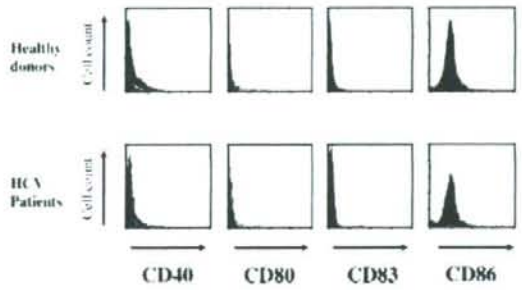

Fig. 1. Fresh myeloid dendritic cells are immature regardless of HCV infection. Myeloid dendritic cells were obtained from HCV-infective patients or healthy donors and their expressions of CD40, CD80, CD83, and CD86 were analyzed by flow cytometry. The shaded histograms are the results with specific Abs, while the open ones are those with isotype Abs. Representative results from five HCV-infected patients and five controls are shown.

IFN-α or PolyI:C Enhanced RIG-I Expression in Myeloid Dendritic Cells

To clarify the factors influencing TLR2, 3, 4, or RIG-I expression in myeloid dendritic cells, it was examined

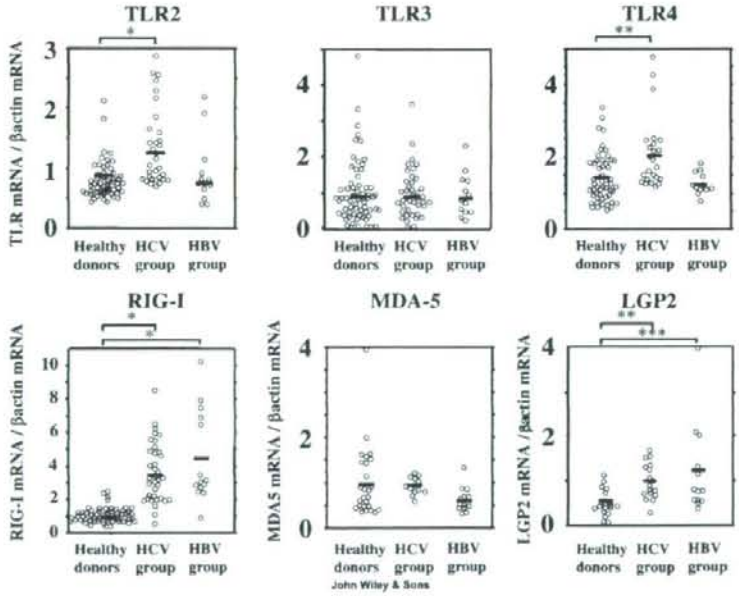

Fig. 2. Expressions of TLR2, TLR4, RIG-I, and LGP2 in patient myeloid dendritic cells from HCV-infected patients are higher than those from healthy donors, while TLR3 and MDA-5 are comparable. Expressions of TLR2, TLR3, TLR4, RIG-I, MDA-5, and LGP2 in myeloid dendritic cells were quantified by real-time RT-PCR as described in Materials and Methods Section. Horizontal bars represent the median. The statistical difference was evaluated by the Mann–Whitney U-test. $^{*}P < 0.0001$, $^{**}P < 0.0005$, $^{***}P < 0.005$.